Cell cycle-dependent expression of AAV2 Rep in HSV-1 co-infections gives rise to a mosaic of cells replicating either AAV2 or HSV-1

Franzoso, Francesca D ; Seyffert, Michael ; Vogel, Rebecca ; Yakimovich, Artur ; de Andrade Pereira, Bruna ; Meier, Anita F ; Sutter, Sereina O ; Tobler, Kurt ; Vogt, Bernd ; Greber, Urs F ; Büning, Hildegard ; Ackermann, Mathias ; Fraefel, Cornel

DOI: https://doi.org/10.1128/JVI.00357-17

Cell cycle-dependent expression of AAV2 Rep in HSV-1 co-infections gives rise to a mosaic of cells replicating either AAV2 or HSV-1

Franzoso, Francesca D; Seyffert, Michael; Vogel, Rebecca; Yakimovich, Artur; de Andrade Pereira, Bruna; Meier, Anita F; Sutter, Sereina O; Tobler, Kurt; Vogt, Bernd; Greber, Urs F; Büning, Hildegard; Ackermann, Mathias; Fraefel, Cornel

Abstract: Adeno-associated virus 2 (AAV2) depends for productive replication on the simultaneous presence of a helper virus such as herpes simplex virus type 1 (HSV-1). At the same time, AAV2 efficiently blocks the replication of HSV-1, which would eventually limit its own replication by diminishing the helper virus reservoir. This discrepancy begs the question how AAV2 and HSV-1 can co-exist in a cell population. Here we show that in co-infected cultures, AAV2 DNA replication takes place almost exclusively in S/G2 cells, while HSV-1 DNA replication is restricted to G1. Live microscopy revealed that not only wtAAV2 replication but also reporter gene expression from both single-stranded and double-stranded (self-complementary) recombinant AAV2 vectors preferentially occurs in S/G2 cells, suggesting that the S/G2 preference is independent of the nature of the viral genome. Interestingly, however, a substantial proportion of the S/G2 cells transduced by the double-stranded but not the single-stranded recombinant AAV2 vectors progressed through mitosis in absence of the helper virus. We conclude that cell cycle-dependent AAV2 rep expression facilitates cell cycle-dependent AAV2 DNA replication, and inhibits HSV-1 DNA replication. This may limit competition for cellular and viral helper factors, and hence, creates a biological niche for either virus to replicate.IMPORTANCE Adeno-associated virus 2 (AAV2) differs from most other viruses, as it requires not only a host cell for replication but also a helper virus such as an adenovirus or a herpes virus. This situation inevitably leads to competition for cellular resources. AAV2 has been shown to efficiently inhibit the replication of helper viruses. Here, we present a new facet of the interaction between AAV2 and one of its helper viruses, herpes simplex virus type 1 (HSV-1). We observed that AAV2 rep gene expression is cell cycle dependent, and gives rise to distinct time controlled windows for HSV-1 replication. High Rep protein levels in S/G2 phases support AAV2 replication and inhibit HSV-1 replication. Conversely, low Rep protein levels in G1 permit HSV-1 replication, but are insufficient for AAV2 replication. This allows both viruses to productively replicate in distinct sets of dividing cells.

DOI: https://doi.org/10.1128/JVI.00357-17

ermann, Mathias; Fraefel, Cornel (2017). Cell cycle-dependent expression of AAV2 Rep in HSV-1 co-infections gives rise to a mosaic of cells replicating either AAV2 or HSV-1. Journal of Virology:e1-e47. DOI: https://doi.org/10.1128/JVI.00357-17

Cell cycle-dependent expression of AAV2 Rep in HSV-1 co-infections gives rise to a mosaic of cells replicating either AAV2 or HSV-1

Francesca D. Franzoso[a], Michael Seyffert[a,b], Rebecca Vogel[a], Artur Yakimovich[c]*, Bruna de Andrade Pereira[a]**, Anita F. Meier[a], Sereina O. Sutter[a], Kurt Tobler[a], Bernd Vogt[a], Urs F. Greber[c], Hildegard Büning[d,e], Mathias Ackermann[a], and Cornel Fraefel[a]#

Institute of Virology, University of Zurich, Zurich, Switzerland[a]; Whitehead Institute for Biomedical Research, Cambridge, USA[b]; Institute of Molecular Life Sciences, University of Zurich, Zurich, Switzerland[c]; Center for Molecular Medicine Cologne, University of Cologne, Cologne, Germany[d]; Institute for Experimental Hematology, Hannover Medical School, Hannover, Germany[e]

Running title: AAV2 and HSV-1 replicate in distinct cells

#Address correspondence to Cornel Fraefel, cornel.fraefel@access.uzh.ch

*Present address: MRC LMCB, University College London, London, United Kingdom;

**Present address: Boehringer Ingelheim Pharma GmbH & Co. KG, Biberach a.d. Riss, Germany;

F.D.F., M.S. and R.V. contributed equally to this work.

ABSTRACT

Adeno-associated virus 2 (AAV2) depends for productive replication on the simultaneous presence of a helper virus such as herpes simplex virus type 1 (HSV-1). At the same time, AAV2 efficiently blocks the replication of HSV-1, which would eventually limit its own replication by diminishing the helper virus reservoir. This discrepancy begs the question how AAV2 and HSV-1 can co-exist in a cell population. Here we show that in co-infected cultures, AAV2 DNA replication takes place almost exclusively in S/G2 cells, while HSV-1 DNA replication is restricted to G1. Live microscopy revealed that not only wtAAV2 replication but also reporter gene expression from both single-stranded and double-stranded (self-complementary) recombinant AAV2 vectors preferentially occurs in S/G2 cells, suggesting that the S/G2 preference is independent of the nature of the viral genome. Interestingly, however, a substantial proportion of the S/G2 cells transduced by the double-stranded but not the single-stranded recombinant AAV2 vectors progressed through mitosis in absence of the helper virus. We conclude that cell cycle-dependent AAV2 *rep* expression facilitates cell cycle-dependent AAV2 DNA replication, and inhibits HSV-1 DNA replication. This may limit competition for cellular and viral helper factors, and hence, creates a biological niche for either virus to replicate.

35 **IMPORTANCE**

36 Adeno-associated virus 2 (AAV2) differs from most other viruses, as it requires not only a
37 host cell for replication but also a helper virus such as an adenovirus or a herpes virus. This
38 situation inevitably leads to competition for cellular resources. AAV2 has been shown to
39 efficiently inhibit the replication of helper viruses. Here, we present a new facet of the
40 interaction between AAV2 and one of its helper viruses, herpes simplex virus type 1 (HSV-
41 1). We observed that AAV2 *rep* gene expression is cell cycle dependent, and gives rise to
42 distinct time controlled windows for HSV-1 replication. High Rep protein levels in S/G2
43 phases support AAV2 replication and inhibit HSV-1 replication. Conversely, low Rep protein
44 levels in G1 permit HSV-1 replication, but are insufficient for AAV2 replication. This allows
45 both viruses to productively replicate in distinct sets of dividing cells.

46 **KEYWORDS** AAV2, HSV-1, helper virus, cell cycle, Rep proteins, biological niche

INTRODUCTION

Viruses depend on host cell factors for the replication of their genome. As the nucleic acid metabolites accumulate during the S phase of the cell cycle, many DNA viruses such as autonomous parvoviruses, adenoviruses, or herpesviruses have evolved mechanisms to manipulate cell cycle progression and induce S or G2 phase arrest, which allows them to replicate their genomes in concert with the cellular DNA (1-3). Herpes simplex virus type 1 (HSV-1) is an enveloped human pathogen with a double-stranded DNA genome of 152 kbp encoding approximately 90 proteins (reviewed in reference (4)). Among those are 7 enzymes, which are essential and sufficient to support HSV-1 DNA replication in cells, and several accessory proteins, including uracyl DNA glycosylase, alkaline exonuclease, thymidine kinase, or ribonucleotide reductase, which are homologous to important cellular S phase proteins. HSV-1 may therefore be less dependent on cellular proteins and a specific phase of the cell cycle. Indeed, unlike many other DNA viruses HSV-1 has been shown to replicate well outside of the S phase and to possess mechanisms for actively arresting cells in G1 and G2 (5-9).

In contrast, adeno-associated virus 2 (AAV2) is a non-pathogenic human parvovirus with a small, single-stranded DNA genome of 4,680 nucleotides. As for herpes viruses, the AAV2 genome is packed in an icosahedral capsid, albeit without a lipid envelope and smaller in size than the herpesvirus capsid. The AAV2 genome contains only two clusters of genes, *rep* and *cap*, flanked by inverted terminal repeats (ITRs), which contain the viral origin of DNA replication and packaging signal. *Cap* gene expression is controlled by the p40 promoter and gives rise to the capsid proteins VP1, VP2, and VP3 which, due to alternative start codons, differ in their N-termini (reviewed in reference (10)). In addition, a nested open reading frame within the *cap* gene encodes a protein designated assembly-activating protein, which is believed to be required for AAV2 capsid assembly in the nucleolus (11). The *rep* gene cluster encodes four Rep isoforms, Rep40, Rep52, Rep68, and Rep78, due to transcription from two different promoters, p5 and p19, and alternative splicing at an intron

near the C-terminus. The multifunctional Rep proteins are involved in diverse processes of the AAV2 life cycle, including DNA replication, regulation of gene expression, genome packaging, and site-specific integration (12-17). The functions of the Rep proteins include site-specific DNA-binding and endonuclease activities (Rep68 and 78), as well as site non-specific ATPase/helicase activity (all Rep isoforms) (18-22). Likely because of its low genetic complexity, AAV2 depends not only on a cell for productive replication, but also on the presence of a helper virus, such as HSV-1, adenovirus 2 (AdV2), or human papillomavirus 16 (HPV16) (23-25). In absence of a helper virus, AAV2 enters cells and establishes a latent infection by maintaining its DNA episomal or inserting it into the host cell genome, preferentially at a site termed AAVS1 on human chromosome 19 (14, 26-28). The dependence of AAV2 on a helper virus inevitably leads to competition for cellular resources and viral factors which are essential for both AAV2 and helper virus replication, such as the HSV-1 ICP8 protein and the helicase/primase complex (29-31). HSV-1 provides also accessory proteins, including the ICP0 protein and the viral DNA polymerase (31), and may condition the cellular environment to promote AAV2 replication, e.g. by interfering with cellular DNA damage signaling (32) or cell cycle progression (5-9, 33).

AAV2 has been demonstrated to efficiently inhibit the replication of its helper viruses human adenovirus type 2 from species C (HAdV-C2) (34-36) and HSV-1 (37, 38). For example, the Rep-mediated inhibition of the protein kinases PKA and PRKX, both members of the cyclic AMP (cAMP) signal transduction pathway, results in decreased expression of cAMP-responsive genes and contributes to Rep-mediated inhibition of AdV replication (39-42). Although the mechanism how AAV2 inhibits HSV-1 replication is less well understood, it also involves the large Rep proteins, in particular the DNA binding and ATPase/helicase activities of Rep68 and 78 (43). We have previously shown that Rep68 can bind to consensus Rep-binding sites located on the HSV-1 genome, and that the Rep helicase domain is sufficient to inhibit DNA replication if binding is facilitated (44). Interestingly however, while the formation of mature HSV-1 replication compartments (RCs) is almost entirely prevented in

cells that support productive AAV2 replication (38), HSV-1 progeny yield from co-infected cultures is only approximately 10-fold lower than in cultures infected with HSV-1 alone (unpublished observation). Because of this observation and the fact that HSV-1 can replicate well in different phases of the cell cycle, we addressed the following two questions: (i) Do HSV-1 provided helper functions allow AAV2 to replicate in different phases of the cell cycle and (ii) do AAV2 and HSV-1 replicate in different sets of cells in co-infected cultures?

The results presented here imply that HSV-1 does not extend its ability to replicate in different phases of the cell cycle to AAV2. In fact, AAV2 gene expression both in presence or absence of the helper-virus and AAV2 replication occur almost exclusively in S/G2 cells. HSV-1 lost its capability to replicate in S/G2 cells in presence of AAV2 *rep* gene expression/DNA replication but still replicated in G1.

RESULTS

For productive infection AAV2 requires a helper virus and a cell in S/G2 phase. We examined the formation of AAV2 replication compartments (RCs) in HeLa Fucci cells which express fluorescent ubiquitination-based cell cycle indicators (Fucci) (45). Specifically, HeLa Fucci cells express green- and red-fluorescent proteins fused to geminin and Cdt1, respectively. In the G1 phase of the cell cycle, geminin undergoes proteasome-dependent degradation and the cells appear red. In the S, G2, and M phases of the cell cycle, Cdt1 is ubiquitinated and degraded; thus, the cells appear green. Cells in early S phase simultaneously express Cdt1 and geminin and appear orange. In early G1, no fluorescence marker is expressed.

In the first set of experiments, HeLa Fucci cells were infected with wtHSV-1 alone or co-infected with wtAAV2 and wtHSV-1. After 24 h viral RCs were visualized by confocal laser scanning microscopy (CLSM) with antibodies specific for the HSV-1 and AAV2 DNA binding proteins ICP8 and Rep, respectively. In cells infected with HSV-1 alone, we detected HSV-1 RCs both in red fluorescent (G1) and green fluorescent (S/G2) cells (Fig. 1, A and C; ratio S/G2:G1 = 1.11 +/- 0.36), which is consistent with previous studies showing that HSV-1 can replicate in G1, S, and G2 phases (5-9). By contrast, AAV2 RCs were identified predominantly in the nuclei of cells expressing the green fluorescent S/G2 phase marker geminin (Fig. 1, B and C; ratio S/G2:G1 = 6.65 +/- 1.01). The S/G2:G1 ratios of total mock-infected HeLa Fucci cells (not gated for RCs) were 1.75 +/-0.10 at 0h p.i. and 1.20 +/- 0.05 at 24 h p.i.; the S/G2:G1 ratios were 1.04 +/- 0.02 in total wtHSV-1 infected and 0.93 +/- 0.02 in wtAAV2 and wtHSV-1 co-infected HeLa Fucci cells. The preference of AAV2 to replicate in the S/G2 phase of the cell cycle was confirmed also by fluorescence in situ hybridization (FISH) with a probe specific for the AAV2 DNA (Fig. 2A). While no FISH signal was detected in non-infected cells (top row), in the cultures infected with wtAAV2 alone, fluorescent dots representing AAV2 genomes were observed in both S/G2 as well as G1 cells (center row). Co-infection with the helper virus supported the formation of AAV2 RCs, and these were

found predominantly in the nuclei of S/G2 cells (bottom row and Fig. 2B). Of note, the AAV2 genomes that have been observed in absence of the helper virus (Fig. 2A, center row) were not visible in the bottom row of Fig. 2A because the laser intensity was strongly reduced for the acquisition of the brightly fluorescent AAV2 RCs. Taken together, these data show that efficient AAV2 replication requires not only the presence of a helper virus but also the cell to be in S/G2 phase of the cell cycle. Therefore, HSV-1 cannot extend its ability to replicate in different phases of the cell cycle to AAV2.

In co-infected cultures HSV-1 DNA replication is inhibited specifically in S/G2 cells. In the previous experiments we monitored cell cycle phases and virus replication in non-gated cells (Fig. 1, A and B; Fig. 2A) and we also determined cell cycle phases of cells "gated" for viral replication markers (Figs. 1C and 2B). Next, we analyzed virus replication in cells gated for cell cycle phase. Specifically, HeLa Fucci cells were infected with wtHSV-1 or co-infected with wtHSV-1 and wtAAV2. After 24 h, cells positive for Cdt1 (G1, red) or geminin (S/G2, green) were sorted by FACS and equal cell equivalents were analyzed by Southern blot, Western blot, and qPCR. Consistent with the findings above, the results of these assays showed that in absence of AAV2, HSV-1 DNA replication was at least as efficient in S/G2 phase as it was in G1 (Fig. 3, A and C), while AAV2 DNA replication in S/G2 was at least 6-fold more efficient than in G1 (Fig. 3, A and D). HSV-1 replication in G1 cells appeared to be equally efficient in presence or absence of AAV2 (Fig. 3, A and C). Interestingly however, in presence of AAV2, HSV-1 DNA was no longer detected by Southern blot in S/G2 cells (Fig. 3A), and qPCR revealed an approximately 4-fold reduction of HSV-1 DNA in S/G2 cells when compared to G1 cells from co-infected cultures and approximately 6-fold reduction when compared to S/G2 cells from cultures infected with HSV-1 alone (Fig. 3C). As infection control, HSV-1 ICP0 and AAV2 Rep proteins were detected by Western blot (Fig. 3B). Of note, the levels of AAV2 DNA appear to directly correlate with the levels of AAV2 Rep proteins in the different cell cycle phases (Fig. 3, A and B). Cell cycle phases of HeLa Fucci cells sorted into G1 (Cdt1, red), early S (Cdt1 and geminin, orange), and S/G2 (geminin,

166 green) populations by FACS were confirmed by DAPI staining and flow cytometry (not
167 shown).

168 These data show that the previously reported AAV2-mediated inhibition of HSV-1 replication
169 (37, 38) is specific to S/G2 phases of the cell cycle and correlates with efficient AAV2
170 replication in these cell cycle phases. The next experiment was performed to investigate
171 whether HSV-1 can replicate in G1 cells despite the presence of AAV2 genomes or simply
172 because AAV2 genomes are absent from those cells. For this HeLa Fucci cells were co-
173 infected with wtAAV2 and a recombinant HSV-1 that encodes ECFP fused with the HSV-1
174 ICP4 protein (rHSV-1vECFP-ICP4) and thus facilitates the observation of HSV-1 RCs due to
175 the binding of the fluorescent ICP4 fusion protein to the replicating HSV-1 DNA in the cell
176 nucleus (46). After 24 h, the cells were fixed and FISH staining was performed using an AF-
177 647 labeled AAV2 DNA probe. The micrographs shown in Fig. 4 demonstrate that HSV-1
178 RCs are formed in G1 cells despite the presence of AAV2 genomes.

179 **Cell cycle dependent AAV2 DNA replication is controlled by cell cycle dependent**
180 **AAV2 *rep* expression.** In absence of a helper virus, gene expression from replication-
181 defective recombinant AAV2 vectors has previously been shown to occur preferentially in
182 the S phase of the cell cycle (47, 48). To address the question whether this applies also
183 when a helper virus is present, we co-infected HeLa Fucci cells with wtHSV-1 and
184 recombinant AAV2 vectors encoding fluorescent reporter proteins fused in frame with AAV2
185 Rep (rAAVCFPRep, rAAVYFPRep). The AAV2 p5 promoter used in these vectors for
186 transcriptional control of reporter gene expression is highly regulated during co-infection; in
187 particular, its activity is very low in absence of HSV-1. Therefore, we also used a
188 recombinant AAV2 vector that expresses a reporter gene from the constitutively active
189 human cytomegalovirus (CMV) IE1 enhancer/promoter (rAAVCFPNeo) to exclude a
190 potential promoter effect responsible for the observed cell cycle dependent AAV2 DNA
191 replication/gene expression. Viral gene expression and cell cycle phase was determined by
192 fluorescence microscopy or flow cytometry. Upon co-infection of HeLa Fucci cells with

rAAVCFPNeo and wtHSV-1, the majority of the cyan-fluorescent cells was indeed in S/G2 phases and approximately 10% in G1 and 10% in early S (Fig. 5, A and B). A similar distribution was observed upon co-infection of HeLa Fucci cells with rAAVCFPRep and wtHSV-1: approximately 81% of the AAV2 transduced (ECFP-positive) cells were in S/G2 phases, while only 19% were in G1, as determined by flow cytometry (Table 1). The inefficient AAV2 gene expression in G1 was observed also in other cell lines, including AT22, HCT116, and NHF (Table 1). For example, in AT22 fibroblast cultures co-infected with rAAVYFPRep and wtHSV-1, more than 80% of AAV2-transduced (EYFP-positive) cells were in S or G2 phases, while only approximately 16% of these cells were in G1 (Table 1), although the majority (approximately 60%) of the non-gated cells in the culture was in G1 phase (not shown). Therefore, HSV-1 helper functions appear to support neither AAV2 replication nor AAV2 (*rep*) gene expression in G1 cells, independent of the promoter, p5 or CMV. Inefficient AAV2 gene expression in G1, and consequently low levels of AAV2 Rep proteins (as indeed observed in Fig. 3B) are likely responsible for the inefficient AAV2 replication and the inefficient inhibition of HSV-1 replication in that cell cycle phase, as AAV2 Rep proteins are known to be essential for AAV2 replication and responsible also for the inhibition of HSV-1 replication (43, 49).

Next, we addressed the question whether in co-infected cultures HSV-1 replication is allowed in the G1 cells and inhibited in the S/G2 cells, because AAV2 *rep* is expressed efficiently only in the S/G2 but not G1 cells. For this, we used a recombinant HSV-1 that encodes the VP16 protein fused with EYFP (rHSV48EYFP; reference (50)). EYFP-VP16 accumulates on the HSV-1 DNA, and hence is a marker for HSV-1 RCs (50, 51). To simultaneously visualize AAV2 Rep, we used rAAVCFPRep which encodes an ECFP-Rep fusion protein from the viral p5 promoter, and allows not only cell cycle-dependent replication of the viral genome in presence of a helper virus but also monitoring AAV2 RCs via interaction of the fluorescent Rep fusion protein with the replicating viral DNA (reference (31); see also Movie S1). As expected, in cultures co-infected with rHSV48EYFP and

220 rAAVCFPRep, HSV-1 RCs and AAV2 RCs were not co-detected in individual cells (Fig. 5C,
221 left). However, in cells co-infected with rHSV48EYFP and rAAVCFPNeo, which encodes
222 ECFP but no AAV2 Rep proteins, yellow fluorescent HSV RCs were readily detected both in
223 ECFP-positive and in ECFP-negative cells (Fig. 5C, right). By using an epifluorescence
224 microscope, cells positive for yellow fluorescent HSV-1 RCs were examined for ECFP
225 fluorescence (Fig. 5D). In the rHSV48EYFP and rAAVCFPRep co-infected cultures, less
226 than 5% of the cells containing HSV-1 RCs were ECFP-Rep positive. In contrast, in the
227 rHSV48EYFP and rAAVCFPNeo co-infected cultures, approximately 50% of the cells
228 containing HSV-1 RCs were positive also for the AAV2 marker ECFP. Since rAAVCFPNeo
229 transduction was observed predominantly in S/G2 phases of the cell cycle (Fig. 5, A and B),
230 these data suggest that AAV2 infection or non-replicating AAV2 DNA *per se* is not sufficient
231 to inhibit HSV-1 replication in S/G2 phases but that *rep* expression is required. This is
232 supported also by a previous finding that UV-inactivated wtAAV2 genomes, which do not
233 express any AAV2 genes, did not inhibit HSV-1 replication (43). In conclusion, cell cycle-
234 dependent AAV2 *rep* expression seems to be responsible for the observed negative
235 correlation between HSV-1 and AAV2 replication efficiencies in different phases of the cell
236 cycle. Low Rep levels in G1 allow HSV-1 but not AAV2 to replicate, while high Rep levels in
237 S/G2 support AAV2 replication and block HSV-1 replication.

238 **Both single-stranded and double-stranded AAV2 vectors predominantly transduce**
239 **cells in S/G2 phases, independent of the presence or absence of a helper virus.** We
240 used two different approaches to test whether the single-stranded nature of the AAV2 DNA
241 plays a role in the cell cycle-dependent AAV2 gene expression: transfection of plasmid
242 cloned AAV2 genomes and infection with self-complementary (sc) recombinant AAV2
243 vectors, which can form a double-stranded DNA by self-annealing and therefore do not
244 depend on second-strand synthesis for viral gene expression. Specifically, HeLa Fucci cells
245 were transfected with plasmids containing *rep*-positive (pAAVCFPRep) or *rep*-negative
246 (pAAVCFPp5) recombinant AAV2 genomes and, 4 h later, mock-infected or infected with

247 wtHSV-1. After 24 h, the cells were examined by CLSM. The results are shown in Fig. 6 and
248 can be summarized as follows: ECFP-fluorescent AAV2 RCs were readily detected both in
249 G1 and in S/G2 cells of cultures transfected with pAAVCFPRep and infected with the helper
250 virus (Fig. 6A). In presence of HSV-1, ECFP-fluorescence was also detected both in G1 and
251 in S/G2 cells of cultures transfected with pAAVCFPp5, but in these cells ECFP-fluorescence
252 was diffuse and AAV2 RCs were not observed because of the absence of *rep* (Fig. 6B). No
253 ECFP-fluorescence was observed in absence of HSV-1, as both plasmids use the helper
254 virus-dependent AAV2 p5 promoter for transgene expression (not shown).

255 To confirm that HSV-1 supported AAV2 DNA replication can indeed take place in G1 when
256 the template is a circular double-stranded DNA, HeLa Fucci cells were transfected with
257 pAAVCFPRep and, 4 h later, mock-infected or infected with wtHSV-1. After 24 h, episomal
258 DNA was prepared from G1 and S/G2 cells according to the method described by Hirt (52)
259 and subjected to qPCR with primers specific for *rep*. The graph in Fig. 6C shows that the
260 relative AAV2 DNA content in G1 cells is 80% larger in presence of the helper virus,
261 presumably because of DNA replication. We then tested whether HSV-1 DNA replication
262 was blocked also in G1 cells, when *rep* is expressed from a plasmid-cloned recombinant
263 AAV2 genome. The graph in Fig. 6D shows that this is clearly the case. The HSV-1 DNA
264 content of ECFP (AAV2) and Cdt1 (G1, red) double-positive HeLa Fucci cells transfected
265 with pAAVCFPRep prior to HSV-1 infection was reduced by more than 60% compared to
266 that of cells transfected with *rep*-negative pAAVCFPp5 plasmid DNA prior to infection with
267 the helper virus. In summary these data show that AAV2 (*rep*) gene expression, AAV2
268 genome replication, and inhibition of HSV-1 replication can take place in G1 cells, when the
269 AAV2 genome is provided as a circular double-stranded rather than a linear single-stranded
270 DNA template.

271 These data suggest that AAV2 second-strand synthesis may be the limiting factor for
272 efficient AAV2 gene expression/genome replication in G1 and accordingly, one would expect
273 that self-complementary AAV2 (scAAV2) vectors would support gene expression in that cell

274 cycle phase. To investigate this possibility, we infected HeLa Fucci cells with scAAVCFP in
275 presence or absence of the helper virus and monitored reporter gene expression (ECFP)
276 and cell cycle phase from 2-20 h after infection (Fig. 7). Indeed, at 20 h after infection, many
277 transgene-positive G1 cells (purple) were observed in scAAVCFP infected cultures in
278 absence of the helper virus (Fig. 7A, left). However, tracking of individual cells over time
279 revealed that the transgene positive G1 cells observed at 20 h after infection originated from
280 cells that became transgene positive in S/G2 and then went through mitosis (arrows in Fig.
281 7A, right panels; see also Movie S2). Occasionally, cells turned transgene positive in G1
282 phase (not shown). Co-infection with wtHSV-1 largely prevented the generation of transgene
283 positive G1 cells (Fig. 7A), presumably because of an HSV-1 mediated G2 arrest (5, 33). As
284 expected from the previous data, the vast majority of the cells infected with the single-
285 stranded AAV2 vector (rAAVCFPNeo) turned transgene positive in S/G2 phase and did not
286 progress through mitosis, independent of the presence or absence of the helper virus (Fig.
287 7A; see also Movie S3). Also as expected from the previous data, transgene positive G1
288 cells were occasionally observed also in rAAVCFPNeo infected cultures in absence of the
289 helper virus. These cells often but not always originated from transgene positive S/G2 cells
290 that progressed to G1, sometimes without division (Fig. 7A). To quantify the observations
291 from live microscopy, we tracked and counted cells over time from the moment AAV2 vector-
292 encoded ECFP-fluorescence became visible. The graph in Fig. 7B shows that more than
293 90% of the cells turned ECFP-positive in S/G2, independent of the genome structure, single-
294 stranded or double-stranded (self-complementary), or the presence or absence of the helper
295 virus. However, in absence of wtHSV-1, ECFP-fluorescent S/G2 cells progressed through
296 mitosis to G1 phase with a significantly higher frequency when infected with scAAVCFP than
297 with rAAVCFPNeo (Fig. 7C).

298 Overall, we conclude that (i) HSV-1 is not capable of extending its ability to replicate in all
299 phases of the cell cycle to AAV2. (ii) Cell cycle dependent AAV2 DNA replication and
300 inhibition of HSV-1 DNA replication is due to cell cycle-dependent AAV2 *rep* expression. (iii)

Second-strand synthesis is likely not responsible for the cell cycle preference because both single-stranded and double-stranded linear AAV2 genomes preferentially transduce cells in S/G2 phases.

DISCUSSION

In this study, we addressed the question how AAV2 and HSV-1 coordinate their replication programs. For this we used a fluorescence microscopy approach scoring different cell cycle stages and viral RCs on a single cell level, and combined the results with biochemical virus replication measurements in isolated cells at the G1 and S/G2 stages. We find that AAV2 replication occurs predominantly in S/G2 phases. Also, AAV2 gene expression was restricted to S/G2 cells both in presence or absence of the helper virus. HSV-1 replication was in turn restricted to G1 cells in co-infected cultures, while it replicated efficiently both in G1 and in S/G2 cells in absence of AAV2 (for an overview see Tables 2 and 3). On the other hand, HSV-1 RCs were readily detected in S/G2 cells transduced with a *rep*-negative recombinant AAV2 vector. Therefore, as Rep proteins are essential for AAV2 replication and have been found to be at least partially responsible for the AAV2 mediated inhibition of HSV-1 replication (38, 43, 44), we conclude that cell cycle dependent AAV2 *rep* expression is responsible for the observed restriction of AAV2 replication to S/G2 cells and HSV-1 replication to G1 cells.

We have previously shown that the AAV2 Rep68/78 proteins, in particular the combined DNA-binding and the ATPase/helicase activities can block HSV-1 DNA replication on the level of DNA synthesis, even in the absence of AAV2 DNA. We also demonstrated that AAV2 Rep68 can bind to consensus Rep-binding sites on the HSV-1 genome, and that the helicase activity can block the replication of any DNA if binding is facilitated (44). However, the conclusion from the present study that the inhibition of HSV-1 replication is limited to S/G2 cells because AAV2 *rep* is expressed efficiently only in that phase inevitably begs for the question of what controls the cell cycle dependent expression of *rep*. Recombinant AAV2 vectors have been reported to transduce cells predominantly in S phase in absence of a helper virus (47, 48). Our finding that HSV-1 provided helper functions do not support AAV2 replication and gene expression in G1, although HSV-1 itself can replicate in G1 and S/G2 and although the HSV-1 protein ICP0 strongly trans-activates AAV2 *rep* expression,

indicates that a step prior to AAV2 transcription may be blocked. One obvious such step is second-strand synthesis. For example, cellular proteins involved in second-strand synthesis such as polymerases or co-factors may not be available at sufficient concentrations in G1. Likewise, factors that block second-strand synthesis such as DNA damage repair proteins may be abundant or activated in G1 but not in S/G2. We demonstrate that AAV2 transcription and replication is efficient in S/G2 as well as in G1 cells when the template is a circular double-stranded rather than a linear single-stranded DNA template, indicating that cell cycle-dependent *rep* expression may indeed be due to cell cycle-dependent second-strand synthesis. However, the circular versus linear state of the two template DNAs as well as the different means of delivery, transfection versus infection, may also affect transcription in a cell cycle-dependent manner, possibilities that were further explored by using scAAV2 vectors. If inefficient second-strand synthesis in G1 was solely responsible for the observed cell cycle-dependent AAV2 replication and gene expression one would expect that scAAV2 vectors, which can form a double-stranded DNA by self-annealing and therefore do not depend on second-strand synthesis for gene expression, can transduce both G1 and S/G2 cells efficiently. Indeed, in scAAV2 vector transduced cell cultures we observed a considerable proportion of AAV2 transgene-positive G1 cells in absence of the helper virus. But interestingly, high-throughput multi-channel time-laps microscopy of cell cycle progression and viral gene expression showed that the majority of the scAAV2 transduced G1 cells originated from scAAV2 transduced S/G2 cells that progressed through mitosis, an event that was observed at a significantly lower rate upon infection with the single-stranded rAAV2 vector (for an overview see Table 3). We hypothesize that rAAV2 vectors, similar to wtAAV2 (53), can induce a cell cycle arrest more efficiently than the scAAV2 vectors because of the single-stranded versus double-stranded nature of the genome. In presence of the helper virus, neither single-stranded nor double-stranded AAV2 vector-transduced cells progressed through mitosis, presumably because of an HSV-1 induced G2 arrest (33). This hypothesis is supported by the finding that co-infection with an ICP0 deletion mutant of HSV-1, which is replication-competent but does not induce a cell cycle arrest in G2 (33),

allowed scAAV2 vector transduced G2 cells but not rAAV2 vector transduced G2 cells to progress through mitosis (data not shown).

The findings in this study may have important implications for AAV2-mediated gene therapy. Both single-stranded and double-stranded AAV2 vectors depend on cells in S/G2 phase for efficient gene expression, which in fact may contribute to their low transduction efficiency, at least in post-mitotic cells. However, when the target cells are mitotically active, the double-stranded AAV2 vectors may be preferred as they allow the cells to go through mitosis while the single-stranded AAV2 vectors do not. On the other hand, scAAV2 vectors have been shown to induce a more robust innate immune response in mouse liver than rAAV2 vectors (54). In any event, it would be interesting to compare the effect of scAAV2 and rAAV2 vectors on specific factors involved in cell cycle regulation, including p53, retinoblastoma protein, cyclin dependent kinases (CDK), and CDK inhibitors.

The observation that both single-stranded and double-stranded AAV2 vectors transduce cells predominantly in S/G2 phases argues against second-strand synthesis as the mechanism responsible for the cell-cycle dependent AAV2 gene expression/DNA replication and inhibition of HSV-1 DNA replication. Nevertheless, the preference of AAV2 to transduce cells in S/G2 phases of the cell cycle may likely be orchestrated by cellular factors other than those involved in second-strand synthesis. In fact, many different cellular proteins are recruited to AAV2 genomes (32, 55-57). Among those, the DNA damage response (DDR) proteins represent a very prominent group and may differentially affect specific phases in AAV2 genome processing, such as circularization, replication and transcription. DNA damage response is closely linked with the cell cycle through checkpoint proteins. Moreover, there is increasing evidence that CDKs, which are the master regulators of cell cycle progression, have a role also in regulation of the DNA damage repair (for reviews see (58-60), thereby coordinating DNA repair and cell cycle progression. For example, it has been shown that CDK1 activity regulates the choice between different double-strand break (DSB)

repair pathways, homologous recombination (HR) and non homologous end joining (NHEJ). In G1, CDK1 activity is low and NHEJ is used while in S/G2/M phases CDK1 activity is high and HR is employed (61, 62). CDK1 activity stimulates HR by promoting generation of the 3' single-stranded DNA ends which are necessary for HR and inhibitory for NHEJ (61-63). It has also been shown that CDK activity is essential for later steps in HR, specifically in the recruitment of Rad51 (64). Functional roles in DNA damage repair pathways have been demonstrated also for other CDKs in complex with cyclins (for a review see (65)).

The licensing factor that allows AAV2 gene expression/DNA replication in S/G2 phase or the inhibitor that blocks it in G1 remains to be identified. Nevertheless, the "partitioning" of the host cell population between the two different viruses is a novel concept of viral adaptation and a fascinating strategy to minimize competition allowing both, AAV2 and HSV-1 to productively replicate, although in distinct sets of cells.

METHODS

Cells. Normal human fibroblasts (NHF) were obtained from X.O. Breakefield, Massachusetts General Hospital, Charlestown, MA, USA. HeLa Fucci cells were a gift from B. Kraus, University of Regensburg, Regensburg, Germany; these cells encode cell cycle specific proteins fused with red fluorescent (Cdt1, G1) or green fluorescent (geminin, S/G2) fusion proteins (45). HCT116 cells were provided by E. Hendrickson, University of Minnesota, Minneapolis, MN, USA. NHF, HeLa Fucci, HCT116 and HeLa (ATCC) cells were cultured in Dulbecco's modified Eagle medium (DMEM) supplemented with 10% fetal bovine serum (FBS), 100 U/ml penicillin G, 100 µg/ml streptomycin, and 0.25 µg/ml amphotericin B (1% AB). AT22 IJE-T yZ5 cells (kindly provided by Y. Shiloh, Tel Aviv University, Tel Aviv, Israel) were cultured in DMEM supplemented with 10% FBS, 1% AB, and 100 µg/ml hygromycin B. Vero cells (ECACC) and 293T cells (kindly provided by J. Neidhardt, University of Zurich, Zurich, Switzerland) were grown in DMEM supplemented with 10% FBS and 1% AB. All cells were maintained at 37°C in a 95% air–5% CO_2 atmosphere. For all infection experiments, virus was allowed to adsorb for 30 min at 4°C before the temperature was shifted to 37°C for 1 h. The cells were then washed with phosphate-buffered saline (PBS) and incubated with DMEM containing 2% FBS and 1% AB at 37°C for the indicated times after infection.

Plasmids and viruses. Wild-type (wt) HSV-1 strain F was provided by B. Roizman (University of Chicago, Chicago, IL). Recombinant HSV-1 encoding ICP4 fused with ECFP (rHSV-1vECFP-ICP4; reference (46)) was obtained from R.D. Everett, University of Glasgow, Glasgow, UK. Recombinant HSV-1 rHSV48EYFP encoding the VP16 protein fused with EYFP was described previously (50). Wt and recombinant HSV-1 were grown and titrated on Vero cells. Plasmid pAAVtCR which contains a recombinant AAV2 genome that lacks the *cap* gene and encodes unmodified Rep40/52 under control of the p19 promoter and Rep68/78 fused at the N terminus with the fluorescent protein mCherry (31) under control of the p5 promoter, was obtained from A. Salvetti (University of Lyon, Lyon,

France). Plasmids containing recombinant AAV2 genomes pAAVCFPRep or pAAVYFPRep were constructed by replacing the mCherry coding sequence in the pAAVtCR plasmid with ECFP or EYFP coding sequences, respectively, as follows: pAAVtCR was treated first with *Bsr*GI and then partially with *Bam*HI, and the 5169 bp fragment was ligated with the 738 bp *Bsr*GI-*Bam*HI fragment containing the ECFP or EYFP coding sequences from pECFP-N2 or pEYFP-N2 (Clontech), respectively. Plasmid pAAVCFPp5, which encodes ECFP from the AAV2 p5 promoter was constructed by replacing the 1885 bp *Bsr*GI-*Swa*I fragment of pAAVCFPRep, which contains the AAV2 Rep coding sequence, with the *Bsr*G1-*Swa*I adaptor oligonucleotide 5'GTACAAGATCGATATTT3'. The recombinant AAV2 genome rAAVCFPNeo was constructed by replacing the EGFP coding sequence in plasmid pAAVGFP (provided by M. Linden, King's College London School of Medicine, London, UK) with the ECFP coding sequence as follows: pECFP-N2 was treated with *Pst*I and *Not*I, and the 768 bp fragment was ligated with the 6417 bp *Pst*I-*Not*I fragment of pAAVGFP. Transgene expression from pAAVCFPNeo is controlled by the human cytomegalovirus IE1 (CMV) enhancer/promoter. Plasmid pscAAVCFP, which encodes the self-complementary recombinant AAV2 genome scAAVCFP, was constructed by replacing the EGFP coding sequence in pscAAVeGFP (kindly provided by J. Neidhardt, University of Zurich, Switzerland) with the ECFP coding sequence. Specifically, a DNA fragment containing the CMV enhancer/promoter-ECFP coding sequence was amplified by PCR from plasmid pCMVeCFP-PolyA (unpublished material) using forward (5'-AAGATATCACTAGTTAGTTATTAATAGTAATCAATTACG-3') and reverse (5'-CCGGTACCA TGCAGTGAAAAAAATGC-3') primers (PCR conditions: 30 sec 98°C, 35x (10 sec 98°C, 45 sec 58°C, 60 sec 72°C), 10 min 72°C), digested with *Spe*I and *Not*I, and ligated between the *Spe*I and *Not*I sites of pscAAVeGFP. Recombinant AAV2 stocks were produced by transient transfection of 293T cells with pDG (66) and either pAAVCFPRep, pAAVYFPRep, pAAVCFPNeo, or pscAAVCFP. Virus stocks were purified by Iodixanol gradient, and titers were determined as described elsewhere (67). WtAAV2 was grown and titrated as described previously (68).

452 **Antibodies.** The following primary antibodies were used: anti-actin (Santa Cruz
453 Biotechnology SC-10731; dilution for Western blotting [WB], 1:10,000), anti-ICP8 (Abcam
454 Ab-20193; dilution for WB, 1:1,000; dilution for immunofluorescence [IF] assay, 1:200), anti-
455 AAV2 Rep (Fitzgerald Industries 10R-A111A; dilution for WB, 1:200; dilution for IF 1:50),
456 anti-ICP0 (ab6513; dilution for WB, 1:2,000). The following secondary antibodies were used:
457 rabbit anti-mouse IgG-horseradish peroxidase (HRP; Sigma A9044; dilution, 1:10,000), goat
458 anti-rabbit IgG-HRP (Sigma A6154; dilution, 1:10,000), goat anti-mouse IgG (H+L)-Alexa
459 Fluor 405 (AF405; Molecular Probes A31556; dilution, 1:500).

460 **Fluorescence-activated cell sorting (FACS) followed by Western blot, Southern blot,**
461 **or quantitative PCR.** For the experiments shown in Fig. 3, a total of $5x10^6$ HeLa Fucci cells
462 were seeded into 10-cm tissue culture plates and 24 h later mock-infected, infected with
463 wtAAV2 (MOI = 8000 genome containing particles per cell) or wtHSV-1 (MOI 3), or co-
464 infected with wtAAV2 (MOI 8000) and wtHSV-1 (MOI 3). After 24 h, cells positive for Cdt1
465 (G1, red) or geminin (S/G2, green) were sorted using a FACSAria III sorter (BD Biosciences)
466 and prepared for Western analysis, Southern blot or quantitative (q)PCR. For Western blot
467 analysis, cells were trypsinized, washed once with PBS, resuspended in 1× loading buffer
468 (4% SDS, 10% β-mercaptoethanol, 20% glycerol, 0.005% bromphenol blue, 0.125 M Tris-
469 HCl, pH 6.8), and boiled for 10 min. Cell lysates were separated, on 10% SDS-
470 polyacrylamide gels and transferred to Protran nitrocellulose membranes (Whatman,
471 Bottmingen, Switzerland). The membranes were blocked with PBS-T (PBS containing 0.3%
472 Tween 20) supplemented with 5% nonfat dry milk for 1 h at room temperature (RT).
473 Incubation with antibodies was carried out with PBS-T supplemented with 2.5% nonfat dry
474 milk. Primary antibodies were incubated overnight at 4°C, while secondary antibodies were
475 incubated for 1 h at RT. Membranes were washed three times with PBS-T for 10 min after
476 each antibody incubation step. HRP-conjugated secondary antibodies were detected with
477 ECL detection reagent (ECL WB blotting systems; GE Healthcare, Zurich, Switzerland). The
478 membranes were exposed to chemiluminescence detection films (Roche Diagnostics,

Rotkreuz, Switzerland). Detection of anti-actin served as a loading control for the lysate. For Southern blot analysis, extrachromosomal DNA was extracted according to a protocol described by Hirt (52). The DNA was separated on 1% agarose gels and transferred to nylon membranes (Amersham Hybond-N+ RPN119B). Hybridization with a digoxigenin (DIG)-labeled probe specific for the AAV2 Rep78- or the HSV-1 UL35-coding sequences, and subsequent detection by an anti-DIG antibody conjugated with alkaline phosphatase and activation with the chemiluminescence substrate CDP Star was performed according to the manufacturer's protocol (Roche, Mannheim, Germany). The DIG-labeled probe was produced with the PCR DIG probe synthesis kit (Roche). For qPCR, total DNA was isolated using the DNeasy Blood & Tissue Kit (Qiagen, Hilden, Germany) according to the manufacturer's protocol. Viral DNA content was quantified by qPCR using the cellular TERT gene as endogenous control (Applied Biosystems, Fostercity, CA, USA) and primers and TaqMan probe specific for the AAV2 Rep78-coding sequence (fw: 5'ATTGACGGAACTCAACGAC3'; rev: 5'CCTCAACCACGTCCTTT3'; TaqMan probe: 5'CATGATCCAGACGGCGGGTGA3') or primers specific for the HSV-1 UL42 gene (fw: 5'CCCTCAAGTTCTTCTTCCTCACG3'; rev: 5'GGAGTCCTGGCTGTCTGTTG3') and SYBR green (Applied Biosystems, Fostercity, CA, USA). AAV2 sequences were amplified at the following conditions: 2 min 50°C, 15 min 95°C, 40x (15 sec 94°C, 30 sec 56°C, 15 sec 72°C). HSV-1 sequences were amplified at the following conditions: 3 min 95°C, 39x (15 sec 95°C, 60 sec 45°C), 10 sec 95°C, 5 sec 65°C, 5 sec 95°C. For the experiments shown in Fig. 7 C and D, $1.5x10^6$ HeLa Fucci cells in 6 cm tissue culture plates were transfected with 0.5 µg of either pAAVCFPRep or pAAVCFPp5 using Lipofectamine LTX as described by the manufacturer (Life Technologies) and, 4 h later, mock-infected or infected with wtHSV-1 (MOI 2) as described in the legend. After 24 h cells positive for the G1 marker Cdt1 (red), or double-positive for the G1 marker and either CFP-Rep or CFP were sorted using a FACSAria III sorter (BD Biosciences). Then, Hirt DNA or total DNA was prepared from the sorted cell populations. To determine the AAV2 DNA content, Hirt DNA was incubated with

506 *Dpn*I prior to the qPCR reaction in order to degrade the transfected input plasmid DNA
507 isolated from *E.coli*. To determine the HSV-1 DNA content, total DNA was used for qPCR.

508 **Microscopy.** For microscopy HeLa or HeLa Fucci cells were seeded onto coverslips (12-
509 mm diameter; Glaswarenfabrik Karl Hecht GmbH & Co. KG, Sondheim, Germany) in 24-well
510 tissue culture plates (5×10^4 cells per well) or, specifically for epifluorescence live cell
511 microscopy, directly into 96-well tissue culture plates (10^4 cells per well) (see also (69). The
512 next day, the cells were infected as indicated in the results section and the Figure legends.
513 For the experiments shown in Fig. 6, the cells were transfected with 0.5 µg of either
514 pAAVCFPRep or pAAVCFPp5 4 h prior to infection. For live cell microscopy of AAV2 gene
515 expression/replication and cell cycle progression (Fig. 5A; Fig. 7A; Movies S1-3), images
516 were acquired every 30 min from 2 to 20 h after infection by automated multi-site multi-
517 channel live epifluorescence microscopy in a time-lapse mode (37° C, 5% CO_2, humidified)
518 using ImageXpress Micro XL (Molecular Devices) and fluorescence filters (Semrock) for
519 ECFP (AAV2), GFP (G2 phase) and TRITC (G1 phase) (69, 70); images were processed by
520 using the Fiji software (71). For standard fluorescence microscopy or CSLM, the cells were
521 washed once with cold PBS at 24 h after infection and then fixed with 3.7%
522 paraformaldehyde in PBS for 10 min at RT. The fixation process was stopped by incubation
523 with 0.1 M glycine for 10 min at RT and washing twice with cold PBS. For
524 immunofluorescence analysis (Fig. 1, A and B), the cells were permeabilized by treatment
525 with pre-cooled (−20°C) acetone for 2 min followed by 3 washing steps with PBS. The cells
526 were blocked for 30 min with 3% bovine serum albumin (BSA) in PBS. For staining, the cells
527 were incubated with antibodies diluted in PBS-BSA (3%) in a humidified chamber at RT in
528 the dark. The coverslips were placed on droplets (40 µl) of primary antibody solution. After
529 incubation for 1 h, the cells were washed three times with PBS and once with H_2O. All
530 coverslips (with and without antibody staining) were embedded in Glycergel
531 (DakoCytomation, Carpinteria, CA) containing DABCO (26 mg/ml; Fluka, Sigma-Aldrich
532 Chemie GmbH, Munich, Germany), and cells were observed using a confocal laser scanning

533 microscope (CLSM; Leica TCS SP2 AOBS; Leica Microsystems, Wetzlar, Germany; Fig. 1,
534 A and B; Fig. 6A and B), an automated epifluorescence microscope using ImageXpress
535 Micro XL (Molecular Devices; Fig. 5A), or a standard fluorescence microscope (Axio
536 Observer inverted microscope, Zeiss AG, Germany, Fig. 5C). To prevent cross talk between
537 the channels for the different fluorochromes, all channels were recorded separately and
538 fluorochromes with longer wavelengths were recorded first.

539 **Flow cytometry**. HCT116, AT22, NHF, or HeLa Fucci cells were seeded into wells of a 12-
540 well tissue culture plate (10^5 cells per well) and 24 h later, co-infected with wtHSV-1 (MOI
541 1.5 for AT22 cells; MOI 3 for all other cell lines) and either rAAVCFPRep or rAAVYFPRep
542 (MOI 1000 for HeLa Fucci cells; MOI 4000 for all other cell lines) as indicated in Table 1. All
543 cells were incubated at 37°C/5% CO_2 in DMEM supplemented with 2% FBS and 1% AB.
544 After 20-24 h, the cells were trypsinized, washed once with PBS, centrifuged for 10 min at
545 1000 *g* and resuspended in 1 ml PBS. The cells were fixed by addition of 2.5 ml EtOH and
546 incubation overnight at -20°C. To determine the cell cycle phases in HCT116, NHF and
547 AT22 cells, DNA was stained for 30 min with DAPI (4′,6′-diamidino-2-phenylindole; 1µg/ml in
548 PBS containing 0.1% Triton-X100) or propidium iodide (PI; 50µg/ml in PBS containing 0.1%
549 Triton-X100 and 0.1mg/ml RNase A) as indicated in Table 1. A minimum of 40,000 events
550 were scored for each sample using a Gallios Flow Cytometer (Beckman Coulter), and data
551 was analyzed using Kaluza® Flow Analysis Software 1.3 (Beckman Coulter).

552 **Fluorescence in situ hybridization (FISH).** FISH was performed essentially as described
553 in Lux et al. (68). Briefly, an approximately 3.9 kb DNA fragment containing the AAV2
554 genome without the inverted terminal repeats was amplified by PCR from plasmid pDG (66)
555 using forward (5'-CGGGGTTTTACGAGATTGTG-3') and reverse (5'-
556 GGCTCTGAATACACGCCATT-3') primers and the following conditions: 30 sec 95°C, 35x
557 (10 sec 98°C, 15 sec 58°C, 75 sec 72°C), 10 min 72°C. Then the PCR product was digested
558 with *Dpn*I to cut the residual template DNA and purified with Pure Link PCR purification kit
559 (Qiagen). The DNA fragment was labeled with 5-(3-aminoallyl)dUTP by nick-translation, and

the incorporated dUTPs were labeled with the amino-reactive Alexa Fluor 647 dye using the ARES DNA labeling kit (Molecular Probes) according to the manufacturer's protocol. HeLa Fucci cells were plated on glass coverslips in 24 well plates at a density of $1.4x10^5$ cells per well and 24 h later mock-infected, infected with wtAAV2 (MOI 4000), or co-infected with wtAAV2 (MOI 4000) and either wtHSV-1 (MOI 3) or rHSV-1vECFP-ICP4 (MOI 3). At 24 h after infection, the cells were washed with PBS, fixed for 30 min at RT with 2% PFA (in PBS) and then washed again with PBS. Then the cells were quenched for 10 min with 50 mM NH_4Cl (in PBS), washed with PBS, permeabilized for 10 min with 0.2% Triton-X100 (in PBS), blocked for 10 min with 0.2% gelatin (in PBS), and washed again with PBS. The hybridization solution (20 µl per coverslip) containing 1 ng/µl of the labeled DNA probe, 50% formamide, 7.3% dextran sulfate, 15 ng/µl salmon sperm DNA and 0.74 x SSC was denatured for 3 min at 95°C and shock cooled on ice. The coverslips with the fixed and permeabilized cells facing down were placed on a drop (20 µl) of the denatured hybridization solution and incubated over night at 37°C in a humidified chamber. (Of note, the cells were not denatured as the AAV2 genome is a single-stranded DNA). The next day, the coverslips were washed 3 times with 2 x SSC at 37°C, three times with 0.1 x SSC at 60°C, and twice with PBS at RT. Then the cells were embedded in ProLong Anti-Fade Mountant (Molecular Probes) and imaged by confocal laser scanning microscopy (CLSM, Leica SP8; Leica Microsystems, Wetzlar, Germany).

ACKNOWLEDGEMENTS

We would like to thank X.O. Breakefield, B. Kraus, E. Hendrickson, Y. Shiloh, J. Neidhardt, B. Roizman, R. Everett, A. Salvetti, and M. Linden for providing reagents and E.M. Schraner for assistance with the preparation of the figures. This work was supported by grants from the Swiss National Science Foundation, No. 31003A_144094/1 and No. 31003A_166668/1, to CF. The authors declare that they have no conflict of interest.

585 **REFERENCES**

586 1. **Adeyemi RO, Pintel DJ.** 2014. Parvovirus-induced depletion of cyclin B1 prevents
587 mitotic entry of infected cells. PLoS Pathog **10:**e1003891.

588 2. **Berk AJ.** 2007. Adenoviridae: The viruses and their replication, p 2355-2394, Fields'
589 virology. Wolters Kluwer/Lippincott Williams & Wilkins, Philadelphia, Pa.; London.

590 3. **Aubert M, Chen Z, Lang R, Dang CH, Fowler C, Sloan DD, Jerome KR.** 2008. The
591 antiapoptotic herpes simplex virus glycoprotein J localizes to multiple cellular
592 organelles and induces reactive oxygen species formation. Journal of Virology
593 **82:**617-629.

594 4. **Taylor TJ, Brockman MA, McNamee EE, Knipe DM.** 2002. Herpes simplex virus.
595 Frontiers in Bioscience **7:**d752-764.

596 5. **Hobbs WE, 2nd, DeLuca NA.** 1999. Perturbation of cell cycle progression and
597 cellular gene expression as a function of herpes simplex virus ICP0. Journal of
598 Virology **73:**8245-8255.

599 6. **Ehmann GL, McLean TI, Bachenheimer SL.** 2000. Herpes simplex virus type 1
600 infection imposes a G(1)/S block in asynchronously growing cells and prevents G(1)
601 entry in quiescent cells. Virology **267:**335-349.

602 7. **Lomonte P, Everett RD.** 1999. Herpes simplex virus type 1 immediate-early protein
603 Vmw110 inhibits progression of cells through mitosis and from G(1) into S phase of
604 the cell cycle. Journal of Virology **73:**9456-9467.

605 8. **Song B, Liu JJ, Yeh KC, Knipe DM.** 2000. Herpes simplex virus infection blocks
606 events in the G1 phase of the cell cycle. Virology **267:**326-334.

607 9. **Song B, Yeh KC, Liu J, Knipe DM.** 2001. Herpes simplex virus gene products
608 required for viral inhibition of expression of G1-phase functions. Virology **290:**320-
609 328.

610 10. **Muzyczka N, Berns KI.** 2001. Parvoviridae: The viruses and their replication. Fields
611 Virology **2:**2327-2346.

11. **Sonntag F, Schmidt K, Kleinschmidt JA.** 2010. A viral assembly factor promotes AAV2 capsid formation in the nucleolus. Proceedings of the National Academy of Sciences of the United States of America **107:**10220-10225.

12. **Chejanovsky N, Carter BJ.** 1989. Mutagenesis of an AUG codon in the adeno-associated virus rep gene: effects on viral DNA replication. Virology **173:**120-128.

13. **Im DS, Muzyczka N.** 1990. The AAV origin binding protein Rep68 is an ATP-dependent site-specific endonuclease with DNA helicase activity. Cell **61:**447-457.

14. **Kotin RM, Menninger JC, Ward DC, Berns KI.** 1991. Mapping and direct visualization of a region-specific viral DNA integration site on chromosome 19q13-qter. Genomics **10:**831-834.

15. **Samulski RJ, Zhu X, Xiao X, Brook JD, Housman DE, Epstein N, Hunter LA.** 1991. Targeted integration of adeno-associated virus (AAV) into human chromosome 19.[erratum appears in EMBO J 1992 Mar;11(3):1228]. EMBO Journal **10:**3941-3950.

16. **King JA.** 2001. DNA helicase-mediated packaging of adeno-associated virus type 2 genomes into preformed capsids. The EMBO Journal **20:**3282-3291.

17. **McCarty DM, Young SMJ, Samulski RJ.** 2004. Integration of adeno-associated virus (AAV) and recombinant AAV vectors. Annual Review of Genetics **38:**819-845.

18. **Smith RH, Kotin RM.** 1998. The Rep52 gene product of adeno-associated virus is a DNA helicase with 3'-to-5' polarity. J Virol **72:**4874-4881.

19. **Wu J, Davis MD, Owens RA.** 1999. Factors affecting the terminal resolution site endonuclease, helicase, and ATPase activities of adeno-associated virus type 2 Rep proteins. Journal of Virology **73:**8235-8244.

20. **Zhou X, Zolotukhin I, Im DS, Muzyczka N.** 1999. Biochemical characterization of adeno-associated virus rep68 DNA helicase and ATPase activities. Journal of Virology **73:**1580-1590.

21. **Yoon-Robarts M, Linden RM.** 2003. Identification of active site residues of the adeno-associated virus type 2 Rep endonuclease. Journal of Biological Chemistry **278:**4912-4918.

22. **Collaco RF, Kalman-Maltese V, Smith AD, Dignam JD, Trempe JP.** 2003. A biochemical characterization of the adeno-associated virus Rep40 helicase. J Biol Chem **278:**34011-34017.

23. **Hoggan MD, Blacklow NR, Rowe WP.** 1966. Studies of small DNA viruses found in various adenovirus preparations: physical, biological, and immunological characteristics. Proceedings of the National Academy of Sciences of the United States of America **55:**1467-1474.

24. **Buller RM, Janik JE, Sebring ED, Rose JA.** 1981. Herpes simplex virus types 1 and 2 completely help adenovirus-associated virus replication. Journal of Virology **40:**241-247.

25. **Walz C, Deprez A, Dupressoir T, Dürst M, Rabreau M, Schlehofer JR.** 1997. Interaction of human papillomavirus type 16 and adeno-associated virus type 2 co-infecting human cervical epithelium. J Gen Virol **78 (Pt 6):**1441-1452.

26. **Kotin RM, Linden RM, Berns KI.** 1992. Characterization of a preferred site on human chromosome 19q for integration of adeno-associated virus DNA by non-homologous recombination. EMBO Journal **11:**5071-5078.

27. **Linden RM, Ward P, Giraud C, Winocour E, Berns KI.** 1996. Site-specific integration by adeno-associated virus. Proceedings of the National Academy of Sciences of the United States of America **93:**11288-11294.

28. **Linden RM, Winocour E, Berns KI.** 1996. The recombination signals for adeno-associated virus site-specific integration. Proceedings of the National Academy of Sciences of the United States of America **93:**7966-7972.

29. **Weindler FW, Heilbronn R.** 1991. A subset of herpes simplex virus replication genes provides helper functions for productive adeno-associated virus replication. Journal of Virology **65:**2476-2483.

30. **Ward P, Falkenberg M, Elias P, Weitzman M, Linden RM.** 2001. Rep-dependent initiation of adeno-associated virus type 2 DNA replication by a herpes simplex virus type 1 replication complex in a reconstituted system. Journal of Virology **75:**10250-10258.

31. **Alazard-Dany N, Nicolas A, Ploquin A, Strasser R, Greco A, Epstein AL, Fraefel C, Salvetti A.** 2009. Definition of herpes simplex virus type 1 helper activities for adeno-associated virus early replication events. PLoS Pathogens **5:**e1000340.

32. **Vogel R, Seyffert M, Strasser R, Oliveira APd, Dresch C, Glauser DL, Jolinon N, Salvetti A, Weitzman MD, Ackermann M, Fraefel C.** 2011. Adeno-Associated Virus Type 2 Modulates the Host DNA Damage Response Induced by Herpes Simplex Virus 1 during Coinfection. Journal of Virology **86:**143-155.

33. **Li H, Baskaran R, Krisky DM, Bein K, Grandi P, Cohen JB, Glorioso JC.** 2008. Chk2 is required for HSV-1 ICP0-mediated G2/M arrest and enhancement of virus growth. Virology **375:**13-23.

34. **Casto BC, Armstrong JA, Atchison RW, Hammon WM.** 1967. Studies on the relationship between adeno-associated virus type 1 (AAV-1) and adenoviruses. II. Inhibition of adenovirus plaques by AAV; its nature and specificity. Virology **33:**452-458.

35. **Casto BC, Atchison RW, Hammon WM.** 1967. Studies on the relationship between adeno-associated virus type I (AAV-1) and adenoviruses. I. Replication of AAV-1 in certain cell cultures and its effect on helper adenovirus. Virology **32:**52-59.

36. **Carter BJ, Laughlin CA, La Maza LMd, Myers M.** 1979. Adeno-associated virus autointerference. Virology **92:**449-462.

37. **Bantel-Schaal U, Zur Hausen H.** 1988. Adeno-associated viruses inhibit SV40 DNA amplification and replication of herpes simplex virus in SV40-transformed hamster cells. Virology **164:**64-74.

38. **Glauser DL, Strasser R, Laimbacher AS, Saydam O, Clément N, Linden RM, Ackermann M, Fraefel C.** 2007. Live covisualization of competing adeno-associated

694 virus and herpes simplex virus type 1 DNA replication: molecular mechanisms of
695 interaction. Journal of Virology **81:**4732-4743.
696 39. **Chiorini JA, Zimmermann B, Yang L, Smith RH, Ahearn A, Herberg F, Kotin RM.**
697 1998. Inhibition of PrKX, a novel protein kinase, and the cyclic AMP-dependent
698 protein kinase PKA by the regulatory proteins of adeno-associated virus type 2. Mol
699 Cell Biol **18:**5921-5929.
700 40. **Di Pasquale G, Stacey SN.** 1998. Adeno-associated virus Rep78 protein interacts
701 with protein kinase A and its homolog PRKX and inhibits CREB-dependent
702 transcriptional activation. J Virol **72:**7916-7925.
703 41. **Schmidt M, Chiorini JA, Afione S, Kotin R.** 2002. Adeno-associated virus type 2
704 Rep78 inhibition of PKA and PRKX: fine mapping and analysis of mechanism.
705 Journal of Virology **76:**1033-1042.
706 42. **Di Pasquale G, Chiorini JA.** 2003. PKA/PrKX activity is a modulator of
707 AAV/adenovirus interaction. EMBO Journal **22:**1716-1724.
708 43. **Glauser DL, Seyffert M, Strasser R, Franchini M, Laimbacher AS, Dresch C,**
709 **Oliveira APd, Vogel R, Büning H, Salvetti A, Ackermann M, Fraefel C.** 2010.
710 Inhibition of herpes simplex virus type 1 replication by adeno-associated virus rep
711 proteins depends on their combined DNA-binding and ATPase/helicase activities.
712 Journal of Virology **84:**3808-3824.
713 44. **Seyffert M, Glauser DL, Tobler K, Georgiev O, Vogel R, Vogt B, Agúndez L,**
714 **Linden M, Büning H, Ackermann M, Fraefel C.** 2015. Adeno-Associated Virus
715 Type 2 Rep68 Can Bind to Consensus Rep-Binding Sites on the Herpes Simplex
716 Virus 1 Genome. Journal of Virology **89:**11150-11158.
717 45. **Sakaue-Sawano A, Kurokawa H, Morimura T, Hanyu A, Hama H, Osawa H,**
718 **Kashiwagi S, Fukami K, Miyata T, Miyoshi H, Imamura T, Ogawa M, Masai H,**
719 **Miyawaki A.** 2008. Visualizing spatiotemporal dynamics of multicellular cell-cycle
720 progression. Cell **132:**487-498.

46. **Everett RD, Sourvinos G, Orr A.** 2003. Recruitment of herpes simplex virus type 1 transcriptional regulatory protein ICP4 into foci juxtaposed to ND10 in live, infected cells. Journal of Virology **77:**3680-3689.

47. **Russell DW, Miller AD, Alexander IE.** 1994. Adeno-associated virus vectors preferentially transduce cells in S phase. Proc Natl Acad Sci U S A **91:**8915-8919.

48. **Russell DW, Alexander IE, Miller AD.** 1995. DNA synthesis and topoisomerase inhibitors increase transduction by adeno-associated virus vectors. Proc Natl Acad Sci U S A **92:**5719-5723.

49. **Glauser DL, Saydam O, Fraefel C.** 2006. Parvovirus replication. Recent advances in DNA virus replication.

50. **Oliveira APd, Glauser DL, Laimbacher AS, Strasser R, Schraner EM, Wild P, Ziegler U, Breakefield XO, Ackermann M, Fraefel C.** 2008. Live visualization of herpes simplex virus type 1 compartment dynamics. Journal of Virology **82:**4974-4990.

51. **La Boissiere S, Izeta A, Malcomber S, O'Hare P.** 2004. Compartmentalization of VP16 in cells infected with recombinant herpes simplex virus expressing VP16-green fluorescent protein fusion proteins. J Virol **78:**8002-8014.

52. **Hirt B.** 1969. Replicating molecules of polyoma virus DNA. Journal of Molecular Biology **40:**141-144.

53. **Hermanns J, Schulze A, Jansen-Db1urr P, Kleinschmidt JA, Schmidt R, Zur Hausen H.** 1997. Infection of primary cells by adeno-associated virus type 2 results in a modulation of cell cycle-regulating proteins. Journal of Virology **71:**6020-6027.

54. **Martino AT, Suzuki M, Markusic DM, Zolotukhin I, Ryals RC, Moghimi B, Ertl HC, Muruve DA, Lee B, Herzog RW.** 2011. The genome of self-complementary adeno-associated viral vectors increases Toll-like receptor 9-dependent innate immune responses in the liver. Blood **117:**6459-6468.

55. **Nash K, Chen W, McDonald WF, Zhou X, Muzyczka N.** 2007. Purification of host cell enzymes involved in adeno-associated virus DNA replication. Journal of Virology **81:**5777-5787.

56. **Cervelli T, Palacios JA, Zentilin L, Mano M, Schwartz RA, Weitzman MD, Giacca M.** 2008. Processing of recombinant AAV genomes occurs in specific nuclear structures that overlap with foci of DNA-damage-response proteins. Journal of cell science **121:**349-357.

57. **Nicolas A, Alazard-Dany N, Biollay C, Arata L, Jolinon N, Kuhn L, Ferro M, Weller SK, Epstein AL, Salvetti A, Greco A.** 2010. Identification of Rep-Associated Factors in Herpes Simplex Virus Type 1-Induced Adeno-Associated Virus Type 2 Replication Compartments. Journal of Virology **84:**8871-8887.

58. **Branzei D, Foiani M.** 2008. Regulation of DNA repair throughout the cell cycle. Nat Rev Mol Cell Biol **9:**297-308.

59. **You Z, Bailis JM.** 2010. DNA damage and decisions: CtIP coordinates DNA repair and cell cycle checkpoints. Trends Cell Biol **20:**402-409.

60. **Trovesi C, Manfrini N, Falcettoni M, Longhese MP.** 2013. Regulation of the DNA damage response by cyclin-dependent kinases. J Mol Biol **425:**4756-4766.

61. **Aylon Y, Liefshitz B, Kupiec M.** 2004. The CDK regulates repair of double-strand breaks by homologous recombination during the cell cycle. The EMBO Journal **23:**4868-4875.

62. **Ira G, Pellicioli A, Balijja A, Wang X, Fiorani S, Carotenuto W, Liberi G, Bressan D, Wan L, Hollingsworth NM, Haber JE, Foiani M.** 2004. DNA end resection, homologous recombination and DNA damage checkpoint activation require CDK1. Nature **431:**1011-1017.

63. **Zhang Y, Shim EY, Davis M, Lee SE.** 2009. Regulation of repair choice: Cdk1 suppresses recruitment of end joining factors at DNA breaks. DNA Repair (Amst) **8:**1235-1241.

64. **Caspari T, Murray JM, Carr AM.** 2002. Cdc2-cyclin B kinase activity links Crb2 and Rqh1-topoisomerase III. Genes & Development **16:**1195-1208.

65. **Lim S, Kaldis P.** 2013. Cdks, cyclins and CKIs: roles beyond cell cycle regulation. Development (Cambridge, England) **140:**3079-3093.

66. **Grimm D, Kern A, Rittner K, Kleinschmidt JA.** 1998. Novel tools for production and purification of recombinant adenoassociated virus vectors. Human Gene Therapy **9:**2745-2760.

67. **Grieger JC, Choi VW, Samulski RJ.** 2006. Production and characterization of adeno-associated viral vectors. Nat Protoc **1:**1412-1428.

68. **Lux K, Goerlitz N, Schlemminger S, Perabo L, Goldnau D, Endell J, Leike K, Kofler DM, Finke S, Hallek M, Buning H.** 2005. Green fluorescent protein-tagged adeno-associated virus particles allow the study of cytosolic and nuclear trafficking. Journal of Virology **79:**11776-11787.

69. **Yakimovich A, Gumpert H, Burckhardt CJ, Lutschg VA, Jurgeit A, Sbalzarini IF, Greber UF.** 2012. Cell-free transmission of human adenovirus by passive mass transfer in cell culture simulated in a computer model. J Virol **86:**10123-10137.

70. **Yakimovich A, Andriasyan V, Witte R, Wang IH, Prasad V, Suomalainen M, Greber UF.** 2015. Plaque2.0-A High-Throughput Analysis Framework to Score Virus-Cell Transmission and Clonal Cell Expansion. PLoS One **10:**e0138760.

71. **Schindelin J, Arganda-Carreras I, Frise E, Kaynig V, Longair M, Pietzsch T, Preibisch S, Rueden C, Saalfeld S, Schmid B, Tinevez JY, White DJ, Hartenstein V, Eliceiri K, Tomancak P, Cardona A.** 2012. Fiji: an open-source platform for biological-image analysis. Nat Methods **9:**676-682.

FIGURE LEGENDS

FIG 1 Co-detection of cell cycle phase and viral replication compartments. (A and B) HeLa Fucci cells were infected with wtHSV-1 (MOI 3) or co-infected with wtAAV2 (MOI 4000) and wtHSV-1 (MOI 3). After 24 h, the cells were fixed and processed for immunofluorescence analysis and CLSM. (A) HSV-1 replication compartments (RCs) were visualized with a primary antibody specific for the HSV-1 major DNA binding protein ICP8 and an AF405-labeled secondary antibody (blue). (B) AAV2 RCs were visualized with a primary antibody specific for the AAV2 Rep proteins and an AF405-labled secondary antibody (blue). Scale bars = 10 µm. Arrowheads in A and B indicate cells positive for HSV-1 or AAV2 RCs and either the red fluorescent G1 marker Cdt1 (I) or the green fluorescent S/G2 marker geminin (II). (C) From the cultures shown in A and B, approximately 30 cells containing HSV-1 or AAV2 RCs (blue) were analyzed for their cell cycle phase (G1, early S, S/G2). The graphs show mean values from six independent experiments; error bars indicate standard deviations of the mean.

FIG 2 Co-detection of cell cycle phase and AAV2 genomes. HeLa Fucci cells were mock-infected, infected with wtAAV2 alone (MOI 4000), or co-infected with wtAAV2 (MOI 4000) and wtHSV-1 (MOI 3). After 24 h, the cells were fixed and processed for fluorescence in situ hybridization (FISH) and CLSM. (A) AAV2 DNA (yellow) was detected with an AF-647 labeled probe as described in Methods. The red and green signals indicate cells in G1 (Cdt1) and S/G2 (geminin) phases, respectively. The orange cells observed in some cultures are in early S phase where they express both Cdt1 and geminin. Areas in the box were enlarged (last column). Scale bars = 10 µm. (B) From the wtAAV2 and wtHSV-1 co-infected cultures shown in A, approximately 30 cells containing AAV2 RCs were analyzed for their cell cycle phase (G1, early S, S/G2). The graph shows mean values from six independent experiments; error bars indicate standard deviations of the mean.

823 **FIG 3** Viral DNA replication in different phases of the cell cycle. HeLa Fucci cells were mock-
824 infected, infected with either wtAAV2 (MOI 8000) or wtHSV-1 (MOI 3), or co-infected with
825 wtAAV2 (MOI 8000) and wtHSV-1 (MOI 3). After 24 h, cells positive for Cdt1 (G1, red) or
826 geminin (S/G2, green) were sorted by FACS and subjected to Southern and Western blot
827 analysis. (A) Southern blot analysis for detection of HSV-1 and AAV2 DNA (equal cell
828 equivalents were loaded in the different lanes; ss=single stranded, rfm=replication form
829 monomer, rfd=replication form dimer). (B) Western blot analysis to control for virus infection
830 (HSV-1 ICP0 and AAV2 Rep; actin was used as a loading control), and (C and D) qPCR to
831 quantify viral DNA. Graphs in C and D show mean values of relative HSV-1 or AAV2 DNA
832 quantities from triplicate experiments; error bars indicate standard deviations of the mean.

833 **FIG 4** Co-detection of AAV2 genomes, HSV-1 RCs, and cell cycle phase. HeLa Fucci cells
834 were co-infected with wtAAV2 (MOI 4000) and rHSV-1vECFP-ICP4 (MOI 3). After 24 h, the
835 cells were fixed and processed for fluorescence in situ hybridization (FISH) and CLSM. (A)
836 AAV2 DNA (yellow) was detected with an AF-647 labeled probe as described in Methods.
837 HSV-1 RCs were detected by the binding of the HSV-1 ECFP-ICP4 fusion protein to the
838 HSV-1 DNA (blue). The red and green signals indicate cells in G1 (Cdt1) and S/G2
839 (geminin) phases, respectively. The area in the box (upper row, merge) was enlarged in the
840 second row and in panel B. Scale bars = 20 µm. (B) The enlargement and sectioning of the
841 HSV-1 RC-positive cell shown in A (box in top row) reveals the subcellular localization of
842 AAV2 genomes (red arrows); for clarity, the red and green channels were omitted.

843 **FIG 5** Cell cycle dependent AAV2 gene expression controls replication of both AAV2 and
844 HSV-1 in co-infected cultures. (A) HeLa Fucci cells were co-infected with rAAVCFPNeo
845 (MOI 4000) and wtHSV-1 (MOI 3). Images were acquired by automated epifluorescence
846 microscopy using ImageXpress Micro XL (Molecular Devices) and fluorescence filters
847 (Semrock) for ECFP (AAV2 gene expression, blue), EGFP (S/G2 phase, green) and TRITC
848 (G1 phase, red). Scale bars = 20 µm. (B) HeLa Fucci cells were co-infected with
849 rAAVCFPNeo (MOI 1000) and wtHSV-1 (MOI 3) and 20 h later cell cycle phase (G1, early S,

S/G2) of rAAVCFPNeo transduced cells was determined by the expression of Ctd1 (red) and geminin (green). 40'000 cells (events) per sample were counted by flow cytometry. The graph shows mean values from triplicate experiments; error bars indicate standard deviations of the mean. (C) HeLa cells were co-infected with rHSV48EYFP (MOI 3) and either rAAVCFPRep (MOI 4000) or rAAVCFPNeo (MOI 4000). After 24 h, cells were examined by using a standard fluorescence microscope; scale bars = 10 µm. (D) From the cultures shown in (C), 50 cells containing yellow fluorescent HSV-1 RCs were analyzed for the presence of AAV2 RCs in rHSV48EYFP and rAAVCFPRep co-infected cultures or ECFP-fluorescence in rHSV48EYFP and rAAVCFPNeo co-infected cultures. The graph shows mean values from triplicate experiments; error bars indicate standard deviations of the mean.

FIG 6 Detection of cell cycle phase, AAV2 gene expression, and virus replication in cells transfected with circular, double-stranded *rep*-positive or *rep*-negative recombinant AAV2 genomes. (A and B) HeLa Fucci cells were transfected with (A) pAAVCFPRep or (B) pAAVCFPp5 and infected with wtHSV-1 (MOI 2) 4 h later. After 24 h, cells were examined by CLSM with filters specific for Cdt1 (G1, red), geminin (S/G2, green), and ECFP (AAV2, blue). The framed areas in A and B are shown at higher magnification on the right. Arrowheads in A indicate cells positive for AAV2 RCs and either the red fluorescent G1 marker Cdt1 (I) or the green fluorescent S/G2 marker geminin (II). Scale bars in A and B = 40 µm (left panels), 10 µm (right panels). (C) HeLa Fucci cells were transfected with pAAVCFPRep and, 4 h later, mock-infected or infected with wtHSV-1 (MOI 2). After 24 h, extrachromosomal DNA was prepared from Cdt1 positive G1 cells (red) and geminin positive S/G2 cells (green), digested with *Dpn*I and subjected to qPCR with primers specific for AAV2 *rep*. (D) HeLa Fucci cells were transfected with pAAVCFPRep or pAAVCFPp5 and infected 4 h later with wtHSV-1 (MOI 2). Total DNA extracted after 24 h from ECFP (AAV2) and Cdt1 (G1, red) or ECFP and geminin (S/G2, green) double-positive cells was subjected to qPCR with primers specific for HSV-1 DNA. Graphs in C and D show mean values of relative DNA

quantities from triplicate experiments, samples were prepared from equal numbers of cells; error bars indicate standard deviations of the mean.

FIG 7 Live cell imaging of cell cycle dependent AAV2 gene expression. (A) HeLa Fucci cells were infected with scAAVCFP (MOI 3000) or rAAVCFPNeo (MOI 3000) in absence or presence of wtHSV-1 (MOI 3) and images were acquired every 30 min from 2-20 h after infection by automated time-lapse (37° C, 5% CO_2, humidified) epifluorescence microscopy using ImageXpress Micro XL (Molecular Devices) and fluorescence filters (Semrock) for ECFP (AAV2 gene expression), GFP (G2) and TRITC (G1). A total of 36 frames was acquired and the frame numbers are indicated. Overview images are shown in the left panels. Two different positions highlighted in each of the overview images (boxes 1 and 2) were enlarged and tracked over time (right panels). Arrows point to cells from the moment ECFP-fluorescence becomes visible. (B and C) HeLa Fucci cells were infected with rAAVCFPNeo (MOI 3000) or scAAVCFP (MOI 3000) in presence or absence of HSV-1 (MOI 3), images were acquired as described above, and AAV2 transgene (ECFP) positive cells were tracked over time. The graph in C shows the percentage of cells that turned ECFP positive either in G1 or in S/G2 phases. The graph in D shows the percentage of transgene positive S/G2 cells progressing to G1 phase. Both graphs show mean values from at least 100 ECFP positive cells tracked on at least 9 different infection and acquisition experiments; error bars indicate standard deviations of the mean.

Franzoso et al., Figure 1

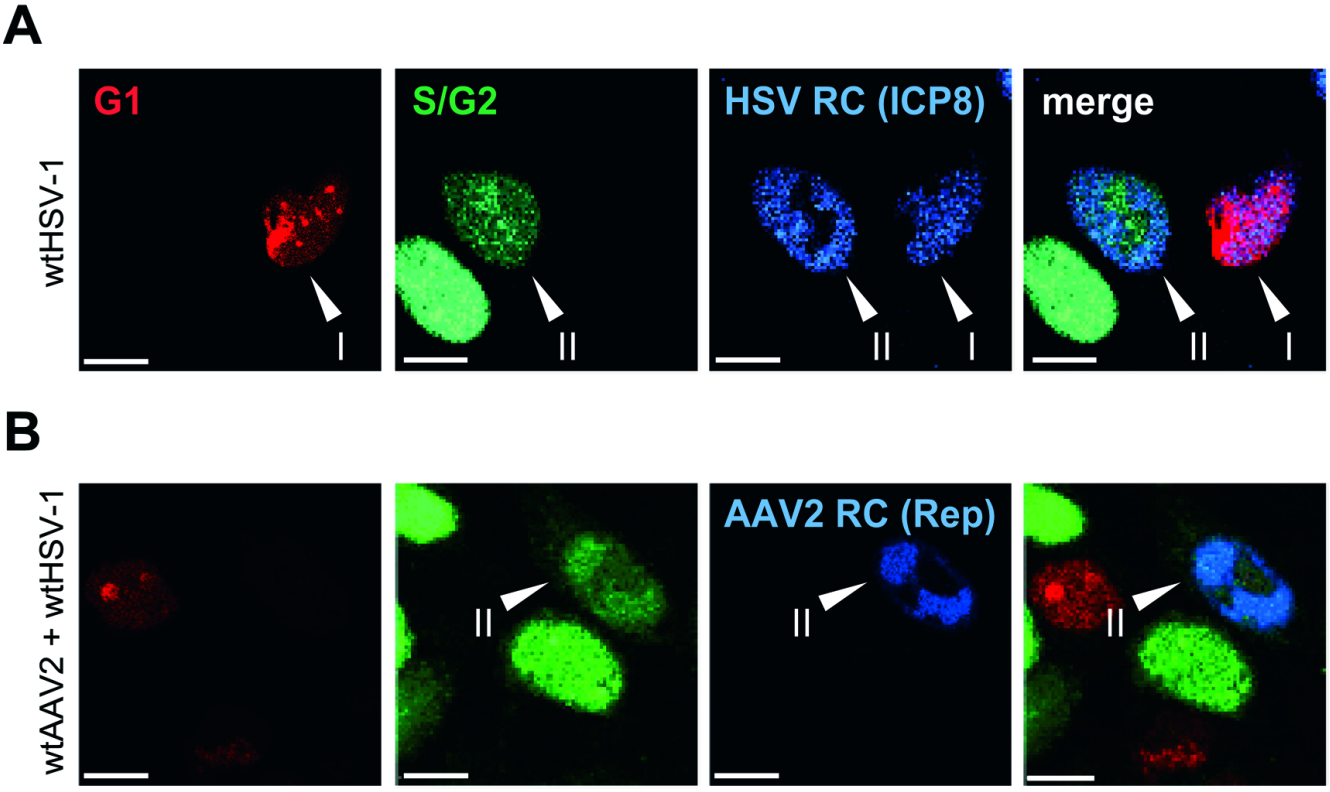

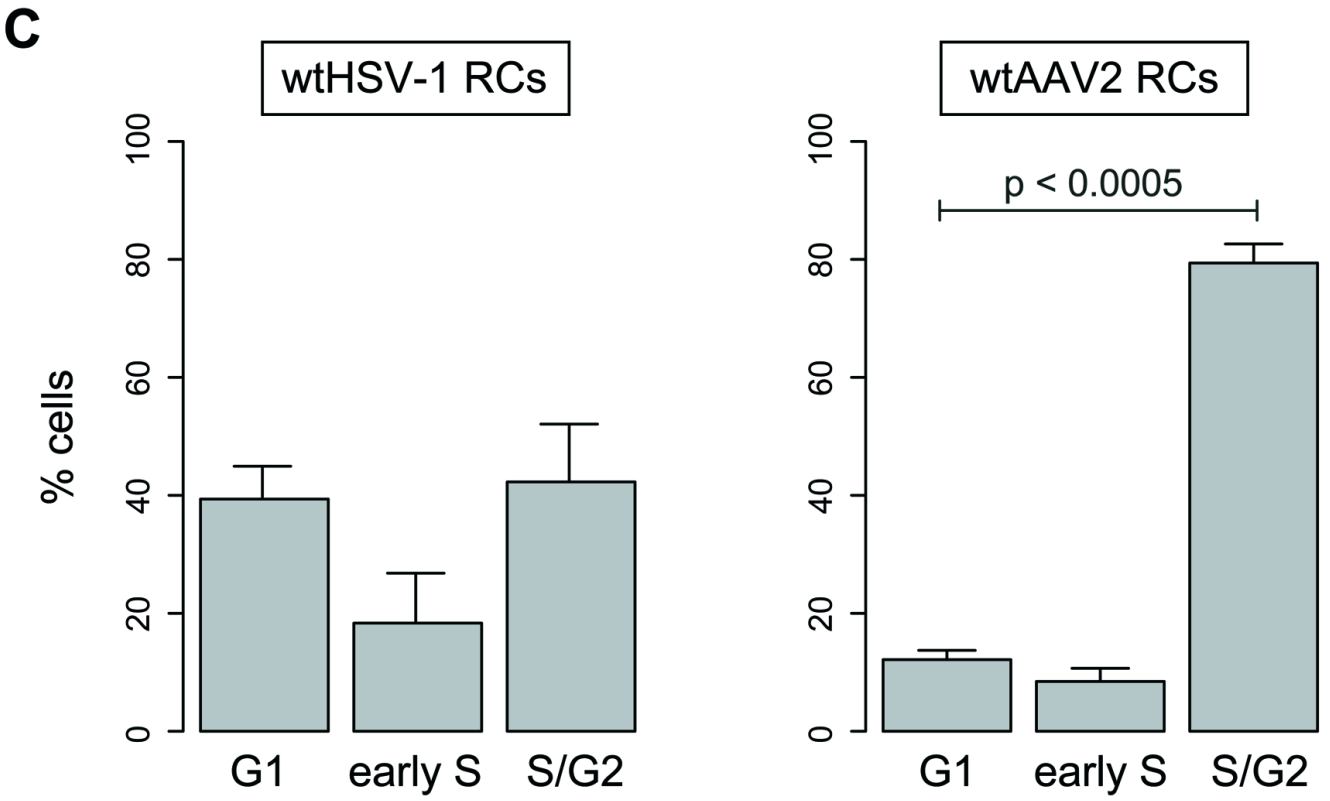

Franzoso et al., Figure 2

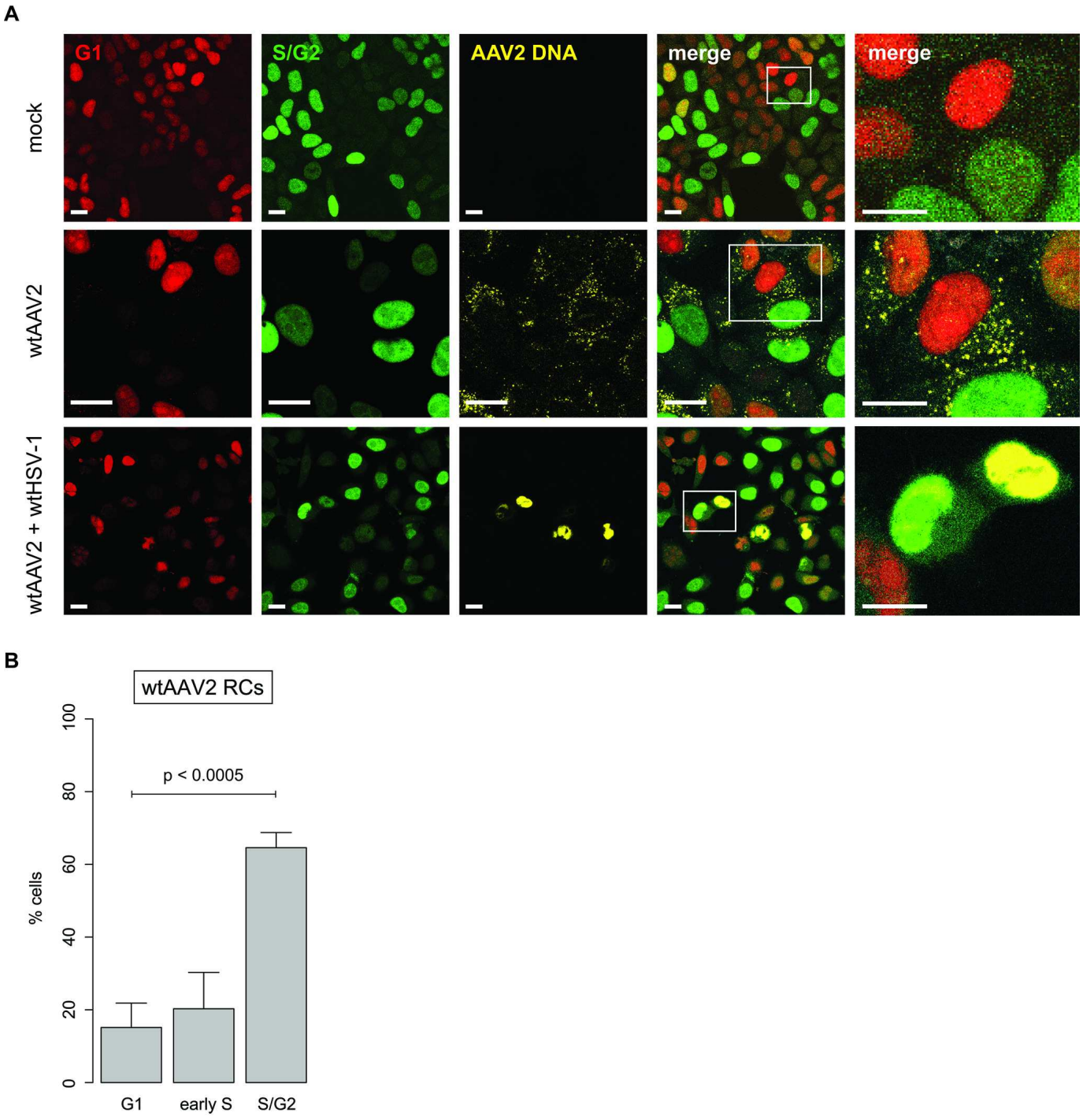

Franzoso et al., Figure 3

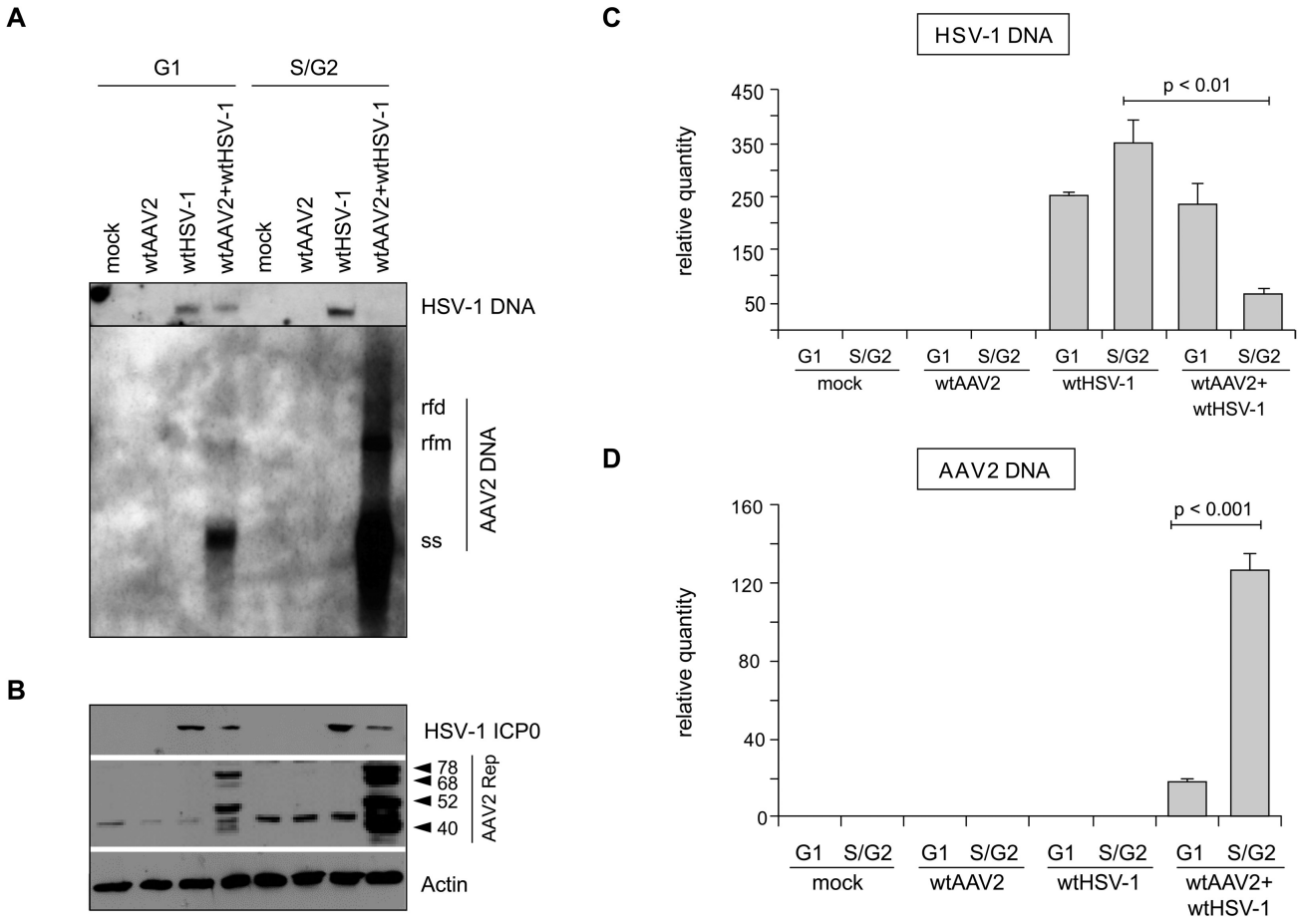

Franzoso et al., Figure 4

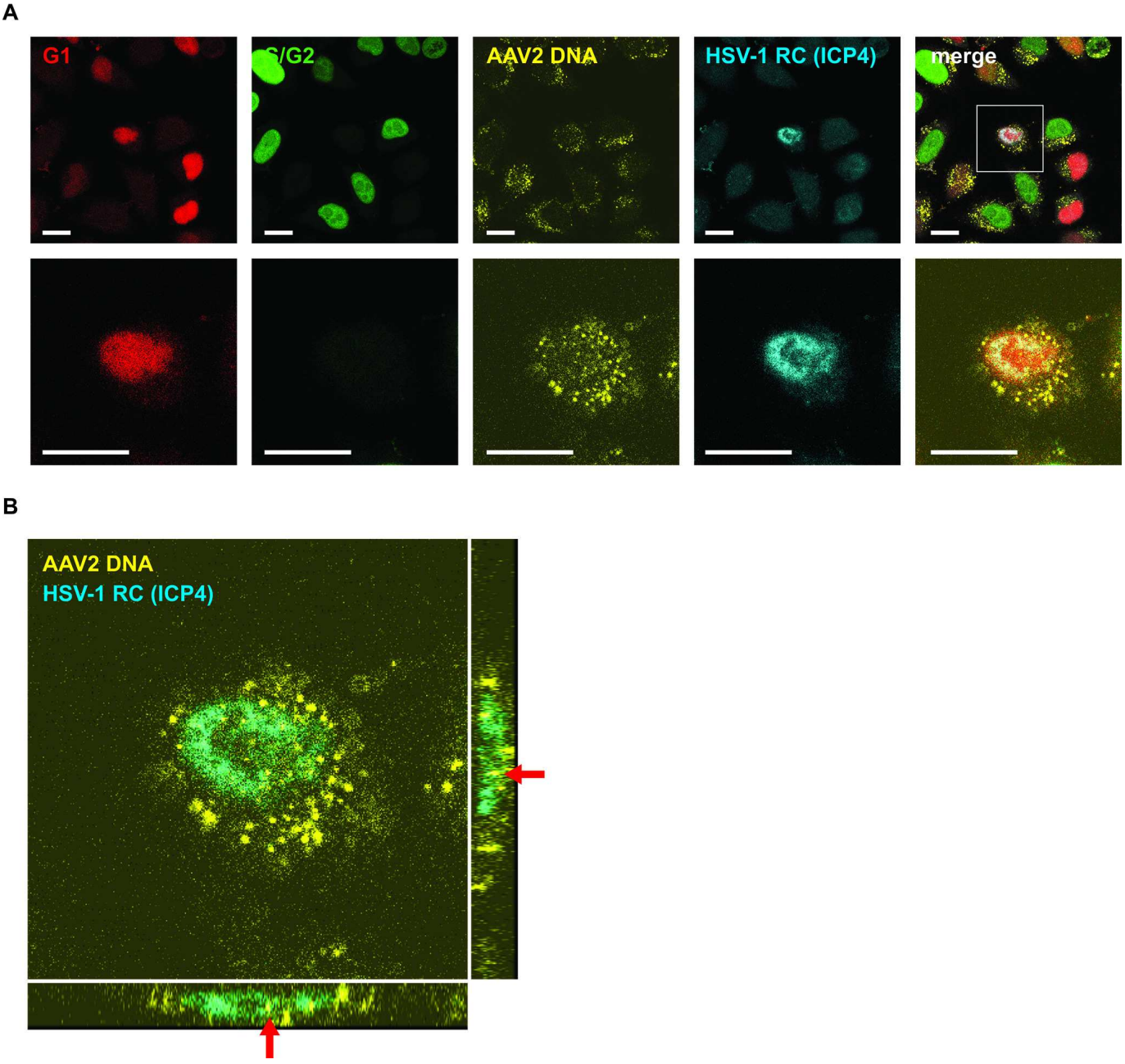

Franzoso et al., Figure 5

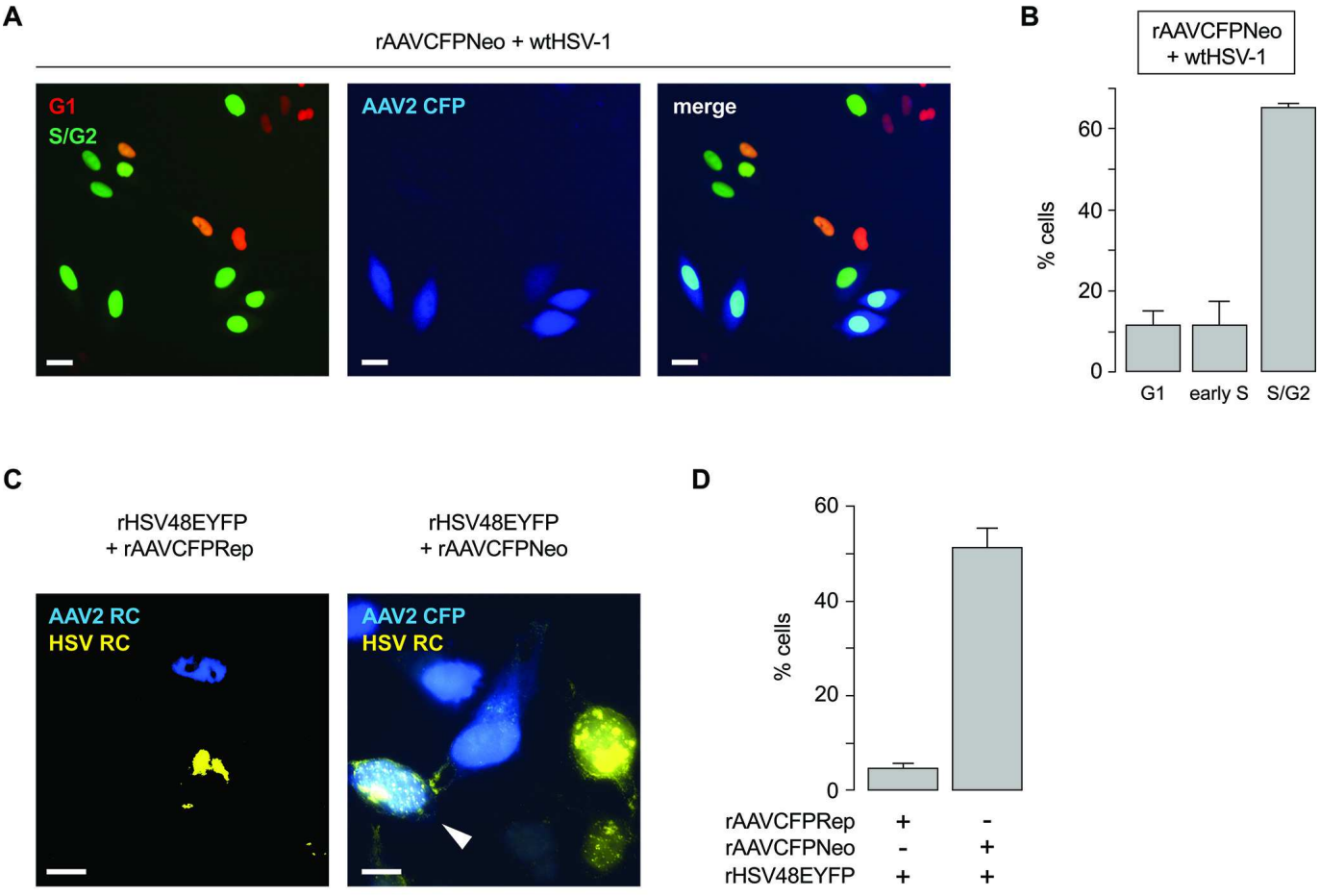

Franzoso et al., Figure 6

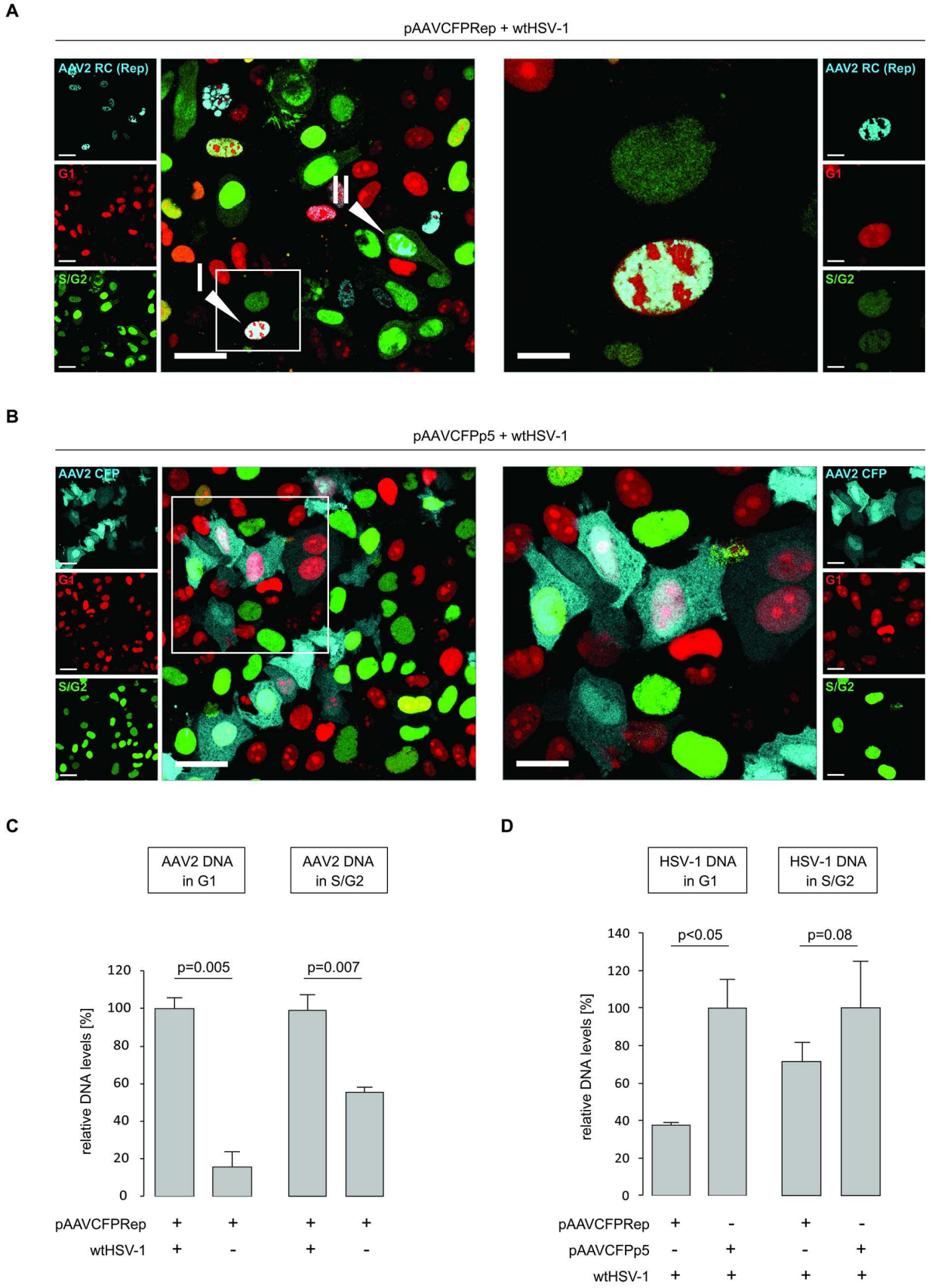

Franzoso et al., Figure 7

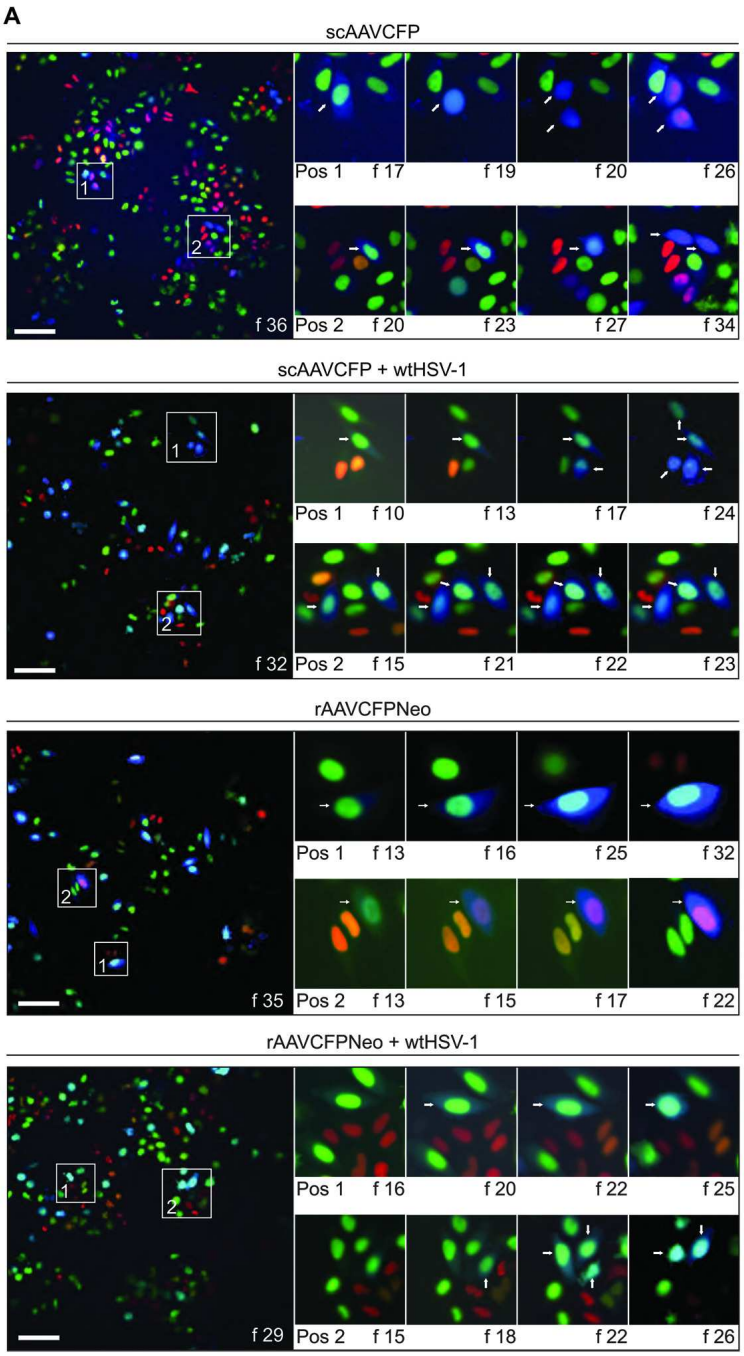

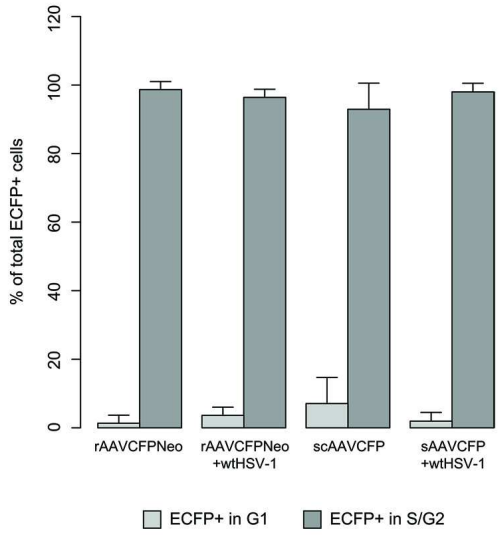

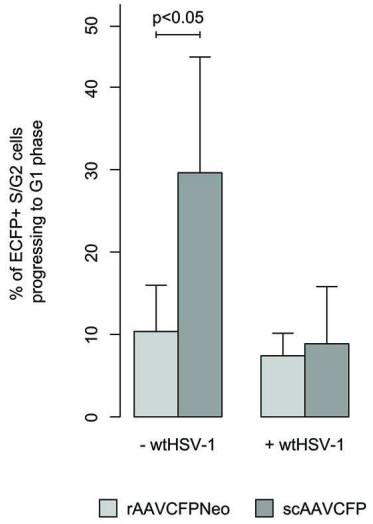

TABLE 1 Cell cycle phases of AAV2 transduced cells.

Cell line	Infection[d]	G1 (%)	S (%)	S/G2 (%)	G2 (%)
HeLa Fucci[a]	rAAVCFPRep	19		81	
AT22[b]	rAAVYFPRep	16	40		44
HCT116[c]	rAAVYFPRep	20	33		47
NHF[b]	rAAVCFPRep	17	35		48

Cell cycle phases were determined by flow cytometry with [a]fluorescent ubiquitination-based cell cycle indicators (Fucci), [b]propidium iodide, or [c]DAPI. [d]Co-infected with HSV-1.

TABLE 2 AAV2 and HSV-1 DNA replication in different cell cycle phases.

Virus infection	G1	S/G2	Illustration
HSV-1	++++	++++	Figs. 1+3
AAV2	-	-	Figs. 2+3
AAV2 (HSV-1 co-infection)	+	++++	Figs. 1-3, Movie S1
HSV-1 (AAV2 co-infection)	++++	+	Figs. 3+4

++++, efficient DNA replication; +, inefficient DNA replication; -, no DNA replication; AAV2 *rep* expression from p5 promoter.

TABLE 3 Cell cycle dependent gene expression from AAV2 vectors and G2-M-G1 transition.

AAV2 vector	Gene expression in G1	Gene expression in S/G2	G2-M-G1 transition	Illustration
ssAAV2cmv	+	++++	+	Fig. 7, Movie S3
ssAAV2cmv (HSV-1 co-infection)	+	++++	+	Figs. 5+7
ssAAV2p5	+	++++	nd	Table 1
dsAAV2cmv	+	++++	++++	Fig. 7, Movie S2
dsAAV2cmv (HSV-1 co-infection)	+	++++	+	Fig. 7

ss, single-stranded; ds, double-stranded; cmv, cytomegalovirus IE1 enhancer/promoter; p5, AAV2 p5 promoter; ++++, efficient gene expression/G2-M-G1 transition; +, inefficient replication/G2-M-G1 transition; nd, not done.